HLA-DR15 Molecules Jointly Shape an Autoreactive T Cell Repertoire in Multiple Sclerosis

Journal Article

Author(s):

Wang, Jian; Jelcic, Ivan; Mühlenbruch, Lena; Haunerdinger, Veronika; Toussaint, Nora Christina (ID); Zhao, Yingdong; Cruciani, Carolina; Faigle, Wolfgang; Foege, Magdalena; Binder, Thomas M.C.; Eiermann, Thomas; Opitz, Lennart; Fuentes-Font, Laura; Reynolds, Richard; Kwok, William W.; Nguyen, Julie T.; Lee, Jar-How; Lutterotti, Andreas; Münz, Christian; Rammensee, Hans-Georg; Hauri-Hohl, Mathias; Sospedra, Mireia; Stevanovic, Stefan; Martin, Roland

HLA-DR15 Molecules Jointly Shape an Autoreactive T Cell Repertoire in Multiple Sclerosis

Graphical Abstract

Highlights

- HLA-DR15 present abundant HLA-DR-derived self-peptides on B cells

- Autoreactive T cells in MS recognize HLA-DR-derived self-peptides/DR15 complexes

- Foreign peptides/DR15 complexes trigger potential autoreactive T cells in MS

- HLA-DR15 shape an autoreactive T cell repertoire by cross-reactivity/restriction
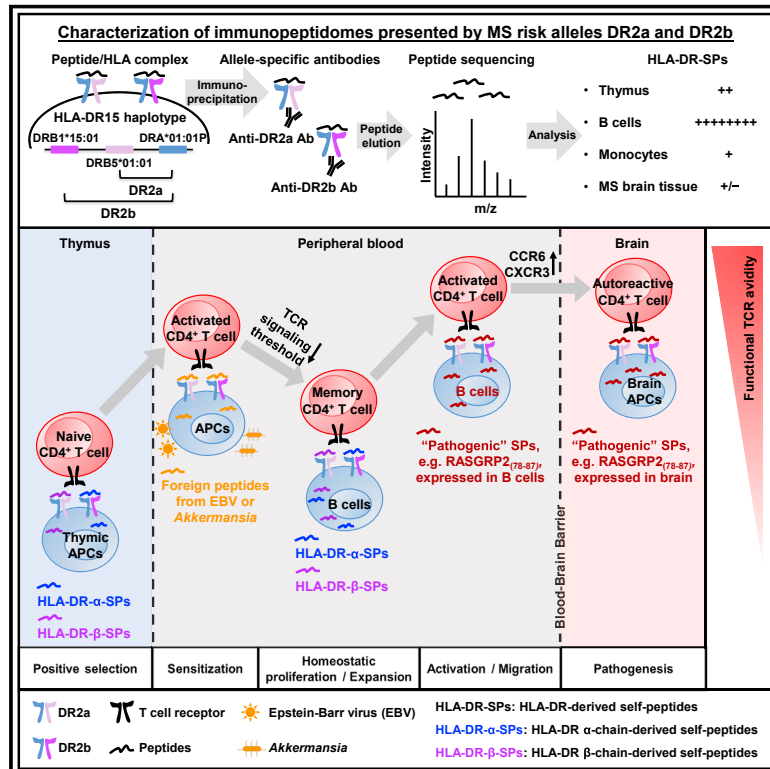
Authors

Jian Wang, Ivan Jelcic,
Lena Mühlenbruch, ..., Mireia Sospedra,
Stefan Stevanovic, Roland Martin

Correspondence

roland.martin@usz.ch

In Brief

The immunopeptidome presented by HLA-DR15 molecules links the most important genetic and environmental risk factors for multiple sclerosis, the HLA-DR15 haplotype and Epstein-Barr virus, by shaping a cross-reactive CD4+ T cell repertoire.

CelPress

Article

HLA-DR15 Molecules Jointly Shape an Autoreactive T Cell Repertoire in Multiple Sclerosis

Jian Wang,[1] Ivan Jelcic,[1] Lena Mühlenbruch,[2,3,4] Veronika Haunerdinger,[5] Nora C. Toussaint,[6,7] Yingdong Zhao,[8] Carolina Cruciani,[1] Wolfgang Faigle,[1] Reza Naghavian,[1] Magdalena Foege,[1] Thomas M.C. Binder,[9] Thomas Eiermann,[10] Lennart Opitz,[11] Laura Fuentes-Font,[12] Richard Reynolds,[12] William W. Kwok,[13] Julie T. Nguyen,[14] Jar-How Lee,[14] Andreas Lutterotti,[1] Christian Münz,[15] Hans-Georg Rammensee,[2,3,4] Mathias Hauri-Hohl,[5] Mireia Sospedra,[1] Stefan Stevanovic,[2,3,4] and Roland Martin[1,16,*]

[1]Neuroimmunology and MS Research, Neurology Clinic, University Hospital Zurich, University of Zurich, Zurich 8091, Switzerland
[2]Department of Immunology, Institute of Cell Biology, University of Tübingen, Tübingen 72076, Germany
[3]German Cancer Consortium (DKTK), Partner Site Tübingen, Tübingen 72076, Germany
[4]Cluster of Excellence iFIT (EXC 2180) "Image-Guided and Functionally Instructed Tumor Therapies," University of Tübingen, Tübingen 72076, Germany
[5]Pediatric Stem Cell Transplantation, University Children's Hospital Zurich, Zurich 8032, Switzerland
[6]NEXUS Personalized Health Technologies, ETH Zurich, Zurich 8093, Switzerland
[7]Swiss Institute of Bioinformatics, Zurich, Switzerland
[8]Biometric Research Program, Division of Cancer Treatment and Diagnosis, NCI, NIH, Rockville, MD 20850, USA
[9]HLA Laboratory of the Stefan Morsch Foundation (SMS), Birkenfeld 55765, Germany
[10]Department of Transfusion Medicine, University Medical Center Hamburg-Eppendorf, Hamburg 20251, Germany
[11]Functional Genomics Center Zurich, Swiss Federal Institute of Technology and University of Zurich, Zurich 8057, Switzerland
[12]Division of Neuroscience, Department of Brain Sciences, Imperial College London, London, UK
[13]Benaroya Research Institute at Virginia Mason, Seattle, WA 98101, USA
[14]One Lambda, Inc., a part of Transplant Diagnostics Thermo Fisher Scientific, 22801 Roscoe Blvd., West Hills, CA 91304, USA
[15]Viral Immunobiology, Institute of Experimental Immunology, University of Zurich, Zurich 8057, Switzerland
[16]Lead Contact
*Correspondence: roland.martin@usz.ch
https://doi.org/10.1016/j.cell.2020.09.054

SUMMARY

The HLA-DR15 haplotype is the strongest genetic risk factor for multiple sclerosis (MS), but our understanding of how it contributes to MS is limited. Because autoreactive CD4^{+} T cells and B cells as antigen-presenting cells are involved in MS pathogenesis, we characterized the immunopeptidomes of the two HLA-DR15 allomorphs DR2a and DR2b of human primary B cells and monocytes, thymus, and MS brain tissue. Self-peptides from HLA-DR molecules, particularly from DR2a and DR2b themselves, are abundant on B cells and thymic antigen-presenting cells. Furthermore, we identified autoreactive CD4^{+} T cell clones that can cross-react with HLA-DR-derived self-peptides (HLA-DR-SPs), peptides from MS-associated foreign agents (Epstein-Barr virus and *Akkermansia muciniphila*), and autoantigens presented by DR2a and DR2b. Thus, both HLA-DR15 allomorphs jointly shape an autoreactive T cell repertoire by serving as antigen-presenting structures and epitope sources and by presenting the same foreign peptides and autoantigens to autoreactive CD4^{+} T cells in MS.

INTRODUCTION

Multiple sclerosis (MS) is the most frequent inflammatory disease of the central nervous system (CNS) in young adults and affects three times more women than men. Autoimmune inflammation, demyelination, and damage to neurons and axons are hallmarks of MS and lead to substantial disability. Together with high treatment costs, MS causes a heavy burden for individuals and society (Reich et al., 2018; Sospedra and Martin, 2005).

The etiology of MS involves environmental influences, such as Epstein-Barr virus (EBV) infection, smoking, and low vitamin D

(Olsson et al., 2017), and genetic risk factors (International Multiple Sclerosis Genetics Consortium, 2018, 2019; Sawcer et al., 2011). The genetic association between the human leukocyte antigen (HLA)-DR15 and MS is the longest known for any autoimmune disease (Jersild et al., 1973) and may contribute up to 60% of the total genetic risk (Oksenberg et al., 2008). The DR15 haplotype contains two DR alleles that give rise to the molecules DRA*01:01P/DRB5*01:01 (or DR2a) and DRA*01:01P/DRB1*15:01 (or DR2b). The genes of the two DR15 allomorphs are in almost complete linkage disequilibrium in Caucasoids (Fogdell et al., 1995). However, it is still widely held that MS
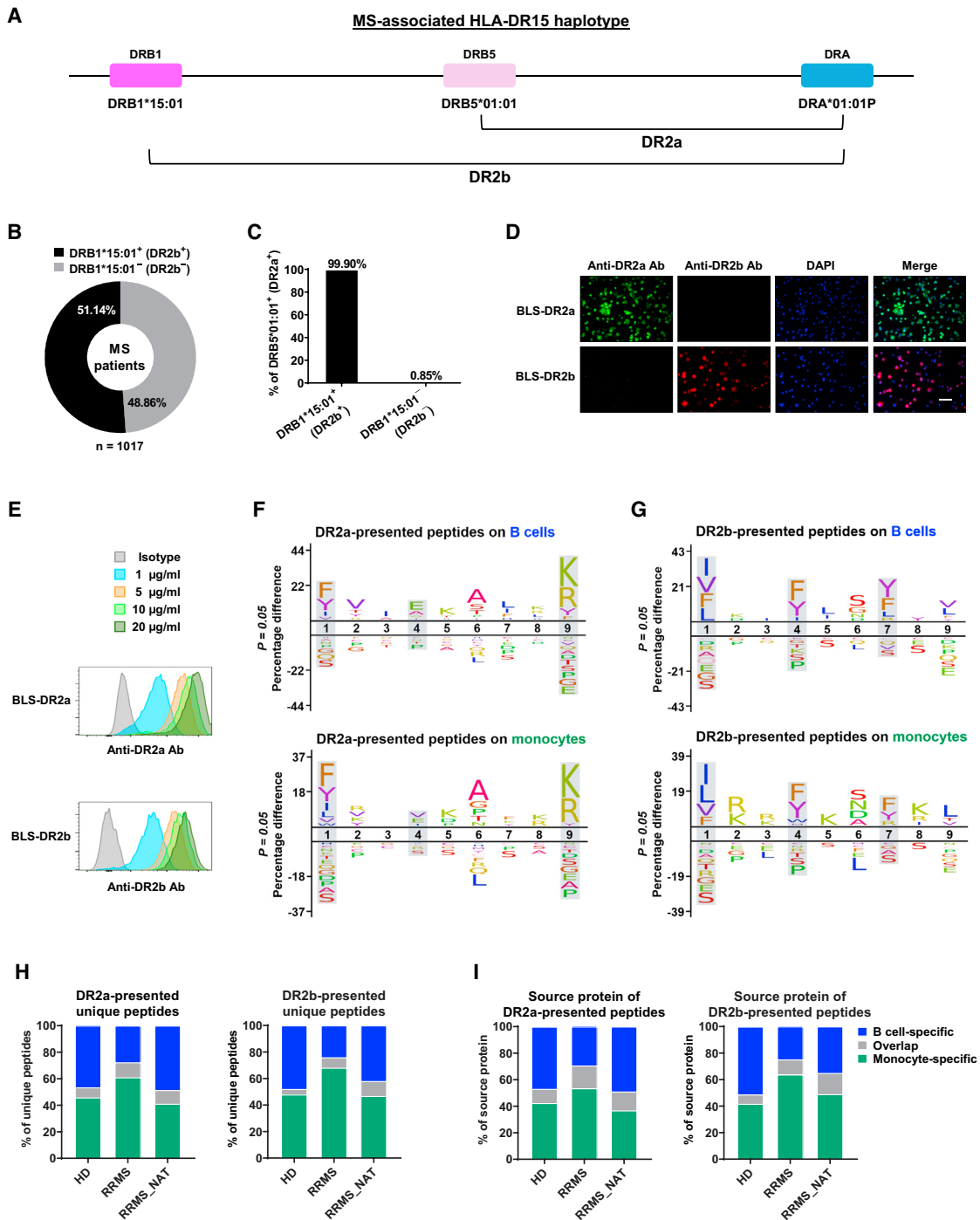
Figure 1. Elution of DR2a- and DR2b-Presented Peptides from Primary B Cells and Monocytes of HLA-DR15+ MS Patients Using Allele-Specific Monoclonal Abs

(A) Genomic organization of HLA-DR loci of the HLA-DR15 haplotype with one HLA-DRA gene (DRA*01:01P) and two HLA-DRB genes (DRB1*15:01 and DRB5*01:01). These genes encode two HLA-DR heterodimers (serotypes) DR2a and DR2b.

(B and C) HLA-DR genotyping results of MS patients (n = 1,017). Proportions of DRB1*15:01+ (DR2b+) and DRB1*15:01− (DR2b−) MS patients (B). Frequencies of DRB1*15:01+ (DR2b+) or DRB1*15:01− (DR2b−) MS patients also carrying the DRB5*01:01 (DR2a) (C).

(D) Cross-reactivity between DR2a and DR2b allele-specific monoclonal Abs was tested using BLS transfectants expressing DR2a (BLS-DR2a) or DR2b (BLS-DR2b) (scale bar, 100 μm).

(legend continued on next page)

risk is solely conferred by DR2b, and in many studies, the influence of DR2a has not been considered; for example, in a recent study of HLA associations with MS (Moutsianas et al., 2015).

How the DR15 haplotype contributes to MS is not fully understood, but several mechanisms have been discussed for MS and other autoimmune diseases (Dendrou et al., 2018), including aberrant HLA class II (HLA-II) molecule expression in an affected tissue (Bottazzo et al., 1983), strong HLA-II molecule expression on antigen-presenting cells (APCs) (Cavalli et al., 2016; Prat et al., 2005), incomplete negative selection of T cells specific for certain autoantigens (Bruno et al., 2002; Klein et al., 2000), and preferential presentation of distinct self-peptides (SPs) and foreign peptides by disease-associated DR molecules to autoreactive CD4$^+$ T cells (Sospedra and Martin, 2005; Sospedra et al., 2006). The best-known example of the latter is the shared epitope hypothesis in rheumatoid arthritis (RA)-associated DR1 and DR4 alleles (Gregersen et al., 1987), which involves better binding of post-translationally modified (citrullinated) SPs (Scally et al., 2013).

Several studies have demonstrated that HLA-derived SPs (HLA-SPs) contribute to HLA-II immunopeptidomes (Chicz et al., 1992, 1993; Rudensky et al., 1991; Vogt et al., 1994). Kourilsky and Claverie (1989) reasoned that major histocompatibility complex (MHC)-derived SPs (MHC-SPs) are involved in thymic selection of T cells and alloreactivity, and others proposed that molecular mimicry between HLA-SPs, foreign antigens, and autoantigens could be involved in autoimmune hepatitis (Burroughs et al., 1992), type 1 diabetes (T1D) (Baum et al., 1995a), and RA (Baum et al., 1995b) based on sequence comparison between peptides from the three different sources. That HLA-SPs from HLA-I and -II molecules can indeed stimulate T cells has been shown by several studies (Chen et al., 1990; de Koster et al., 1989; Mohme et al., 2013). Albani et al. (1995) noted that peptides with the sequence QKRAA derived from DR molecules with the shared epitope in RA exist in the *E. coli* and human heat shock protein DnaJ and can be recognized by synovial fluid-infiltrating T cells in RA.

Accordingly, DR15 molecules and their immunopeptidomes might act in MS at multiple steps, including thymic selection of autoreactive T cells, maintenance/expansion in the periphery, activation by peptides from MS-associated pathogens, and by presenting disease-relevant autoantigens in the brain. This speculation is supported in part by earlier findings that memory B cells and the SPs presented by DR15 molecules can be involved in increased autoproliferation and brain homing of autoreactive CD4$^+$ T cells in MS (Jelcic et al., 2018; Mohme et al., 2013).

Certain infections, particularly with EBV, are thought to lead to marked immune activation and stimulate autoreactive T cells via molecular mimicry between foreign agents and myelin peptides (Wucherpfennig and Strominger, 1995). EBV establishes latent infection in B cells and drives their activation and differentiation, which might contribute to MS pathogenesis as APCs or via proinflammatory cytokines and antibodies (Lünemann et al., 2007). Interestingly, the DR15 haplotype alone increases MS risk approximately 3-fold and 15-fold together with environmental risk factors (Olsson et al., 2017).

Thus, the present study aimed to address how the immunopeptidomes presented by both DR15 allomorphs, DR2a and DR2b, on different APCs in the thymus, peripheral blood, and brain could be involved in shaping an autoimmune T cell repertoire and how environmental triggers might contribute to activating potentially autoreactive CD4$^+$ T cells.

RESULTS

DR2a and DR2b Immunopeptidomes on Primary B Cells and Monocytes

The virtually complete linkage disequilibrium of the two DR15 allomorphs (Figure 1A) was highlighted by HLA genotyping over 1,000 MS patients (Figure 1B). 51.14% of them were DRB1*15:01$^+$, and, as shown previously (Fogdell et al., 1995), 99.90% of DRB1*15:01$^+$ MS patients were also DRB5*01:01$^+$ (Figure 1C). Very rarely (0.85%), DRB5*01:01 could be found in DRB1*15:01$^-$ individuals (Figure 1C; Robbins et al., 1997). Thus, both DR15 allomorphs should be considered when examining genetic risk factors and how they influence cellular immunity in MS.

Several studies have shown, albeit indirectly, the importance of memory B cells as cytokine producers and APCs in MS and its animal model (Hauser et al., 2008; Jelcic et al., 2018; Li et al., 2015; Molnarfi et al., 2013; Sabatino et al., 2019). We therefore focused on immunopeptidomes of peripheral blood B cells and another type of prominent APCs: monocytes. High-affinity, allele-specific immunoglobulin G (IgG) antibodies were generated to isolate peptide/DR2a and peptide/DR2b complexes (Figure S1A). Both antibodies displayed high specificity and affinity for the respective DR15 molecule (Figures 1D, 1E, and S1B). The DR15$^+$ donors, including 3 healthy donors (HDs), 3 untreated relapsing-remitting MS (RRMS) patients, and 3 RRMS patients treated with the anti-VLA4 antibody natalizumab (RRMS_NAT) (Table S1) were chosen for immunopeptidome analyses. These donors did not express other DR alleles that could be recognized by the two allele-specific antibodies (Figure S1B; Table S1). RRMS_NAT patients were of interest because of increased number and activation of blood B cells (Planas et al., 2012) and elevated autoproliferation of T and B cells (Jelcic et al., 2018). Flow cytometry testing with anti-DR2a and anti-DR2b antibodies showed comparable expression levels of DR2a and DR2b on B cells and monocytes in HDs and MS patients (Figure S1C) but higher DR2a expression on both cell types (Figure S1D), as

---

(E) Binding affinities of DR2a or DR2b allele-specific monoclonal Abs. The x axis indicates fluorescence intensity.
(F and G) 9 amino acid binding motifs of DR2a-presented (F) and DR2b-presented (G) peptides on B cells and monocytes based on NetMHCII 2.3 analysis and visualization by iceLogo. Putative peptide anchor positions for DR2a and DR2b are highlighted in gray.
(H) Overlap of the DR2a- or DR2b-presented unique peptides between B cells and monocytes at the group level (HDs, n = 3; RRMS, n = 3; RRMS_NAT, n = 3).
(I) Overlap of the source proteins of DR2a- or DR2b-presented peptides between B cells and monocytes at the group level (HDs, n = 3; RRMS, n = 3; RRMS_NAT, n = 3).
See also Figures S1 and S2 and Tables S1, S2, and S3.

observed previously using allele-specific IgM antibodies (Prat et al., 2005).

Next we analyzed DR2a and DR2b immunopeptidomes of B cells and monocytes by isolating peptide/DR2a and peptide/DR2b complexes with the allele-specific antibodies and subsequent liquid chromatography-tandem mass spectrometry (LC-MS/MS). Comparison of unique (Figure S2A) and total peptides showed no significant difference for DR2a-presented unique peptides between B cells and monocytes (Figure S2B; Table S2), but the total eluted peptides from DR2a on RRMS_NAT B cells was higher compared with RRMS B cells and RRMS_NAT monocytes (Figure S2B), probably because of higher numbers of activated blood B cells in RRMS_NAT (Planas et al., 2012). Comparison of DR2b-presented peptides showed no significant difference between groups, only lower unique and total peptides on RRMS B cells compared with RRMS monocytes (Figure S2C; Table S3). Thus, in general, the diversity of unique peptides and their total numbers on DR2a or DR2b are comparable for B cells and monocytes and for HDs and MS patients. Further, the deduced amino acid preferences at the DR anchor positions p1, p4, and p9 for DR2a or p1, p4, and p7 for DR2b (Vogt et al., 1994) were largely similar for B cells and monocytes (Figures 1F and 1G), but differences at other positions implied different peptide sources of DR2a- or DR2b-presented peptides on B cells and monocytes.

DR2a and DR2b Immunopeptidomes on B Cells Are Skewed toward HLA-DR-SPs

Comparison of DR2a- or DR2b-presented peptides and source proteins between B cells and monocytes showed limited overlap, indicating cell-type-specific immunopeptidomes (Figures 1H, 1I, and S2D–S2G). Likely explanations are the different protein expression profiles (Figure S2H) and/or differences in proteolytic enzymes in the antigen-processing compartments (Villadangos and Ploegh, 2000; Figure S2I). Interestingly, ∼50% of the DR2a-presented peptides on B cells were HLA-SPs, particularly from HLA-II molecules (HLA-II-SPs), but much fewer HLA-SPs were found on DR2a of monocytes (Figures 2A and 2B), which also applied to DR2b-presented HLA-SPs (Figures 2C and 2D). Thus, DR2a and DR2b immunopeptidomes on B cells are enriched for HLA-SPs.

Considering the role of B cells in MS, we examined the source of the HLA-II-SPs in B cells in more detail. DR2a- and DR2b-presented HLA-II-SPs were mainly derived from DR molecules (HLA-DR-SPs) (Figures 2E and 2F, left panels), and DR2a preferentially presented SPs from DR β chains (HLA-DR-β-SPs), particularly from DRB1 and DRB5 (Figure 2E, right panel), whereas DR2b preferentially presented SPs from DR α chains (HLA-DR-α-SPs) (Figure 2F, right panel).

Among the B cell-presented HLA-DR-SPs, five peptides were particularly prominent. Four were mainly found on DR2a, including DRB1$_{(57–70)}$, DRB1$_{(72–86)}$, DRB5$_{(72–86)}$, and DRB1/5$_{(184–199)}$. The remaining one, DRA$_{(70–85)}$, was more abundant on DR2b (Figures 2G and S3A). Interestingly, all five could originate from DR2a and DR2b themselves (Figure 2G; Tables S2 and S3). Thus, on B cells of DR15$^+$ individuals, DR2a and DR2b serve as antigen-presenting molecules and, at the same time, as an epitope source. We then examined whether presen-

tation of these five HLA-DR-SPs was a general phenomenon or limited to certain APCs/tissues by analyzing the immunopeptidomes presented in the thymus from immunologically healthy DR15$^+$ individuals and in the target organ of MS, the brain, of DR15$^+$ MS patients (Table S4). For the latter, we chose highly inflamed tissue samples. The five HLA-DR-SPs were also present in the DR2a and DR2b immunopeptidomes of thymic tissues but not MS brain tissues (Figure 2H).

The differential abundance of HLA-DR-SPs on DR2a and DR2b likely depends on the binding affinity to the respective allele. Among the DR2a-presented HLA-DR-SPs, DRB1$_{(72–86)}$ was most frequent, followed by DRB1/5$_{(184–199)}$, DRB5$_{(72–86)}$, and DRB1$_{(57–70)}$ (Figure S3A). This order corresponded to predicted binding affinities to DR2a (Figure S3B), which were much higher than those to DR2b (Figure S3C). Conversely, the DR2b-presented peptide DRA$_{(70–85)}$ had a much higher predicted binding affinity to DR2b than DR2a (Figure S3C). Although at much lower frequency, HLA-DR-β-SPs were also eluted from DR2b and, vice versa, the HLA-DR-α-SPs from DR2a in 8 of 9 individuals (Figures S3D and S3E), indicating that their differential presentation is not strictly limited to one of the two DR15 allomorphs. Regarding the location of HLA-DR-SPs within the HLA-DR molecules, DRA$_{(70–85)}$ was from the non-polymorphic DRA, whereas the four HLA-DR-β-SPs were from polymorphic areas of the DR β chains (Figure S3F). Next we wondered how frequently these peptides had been identified in the immunopeptidomes of DRB1*15:01$^+$ individuals versus those carrying other DR types in immunopeptidomes of over 600 samples from tumors, unaffected surrounding tissue, and blood samples in the HLA Ligand Atlas (Marcu et al., 2019). Each of the five HLA-DR-SPs had also been identified in DRB1*15:01$^-$ samples, but at much lower frequency than in DRB1*15:01$^+$ (Figure S3G). However, the anti-pan-HLA-DR (L243) and anti-DR/DP/DQ (Tü39) antibodies had been used in these studies, and, thus, the origin of the HLA-DR-SPs from DR2a or DR2b could not be assigned. These results suggest that HLA-DR-SPs are more common in DR15$^+$ individuals.

Memory CD4$^+$ T Cells in HLA-DR15$^+$ MS Patients Respond to HLA-DR-SPs

Because increased autoproliferation of CD4$^+$ T cells in MS is mediated by B cells and depends on T cell receptor (TCR)-peptide/DR interactions (Jelcic et al., 2018), we hypothesized that the surface expression of DR2a and DR2b on B cells and the nature of HLA-DR-SPs might be important. Indeed, there is a tendency of higher autoproliferation with increasing HLA-DR-SPs presented by DR2a and DR2b on B cells from MS patients (Figure S4A). We then tested CD4$^+$ T cell responses against these HLA-DR-SPs (Table S5) in DR15$^+$ HDs and MS patients. We used CD45RA-depleted (CD45RA$^-$) peripheral blood mononuclear cells (PBMCs), which include monocytes and memory T cells (CD4$^+$ and CD8$^+$) but not B and naive T cells (Figure S4B) to reduce background autoproliferation (Jelcic et al., 2018; Mohme et al., 2013; Figure S4C). CD45RA$^-$ PBMCs of 8 HDs and 14 MS patients (4 RRMS and 10 RRMS_NAT) (Table S1) were tested with individual or pooled HLA-DR-SPs. Interestingly, cells of MS patients responded robustly to individual and pooled HLA-DR-SPs, whereas HDs responded much less (Figure 3A).
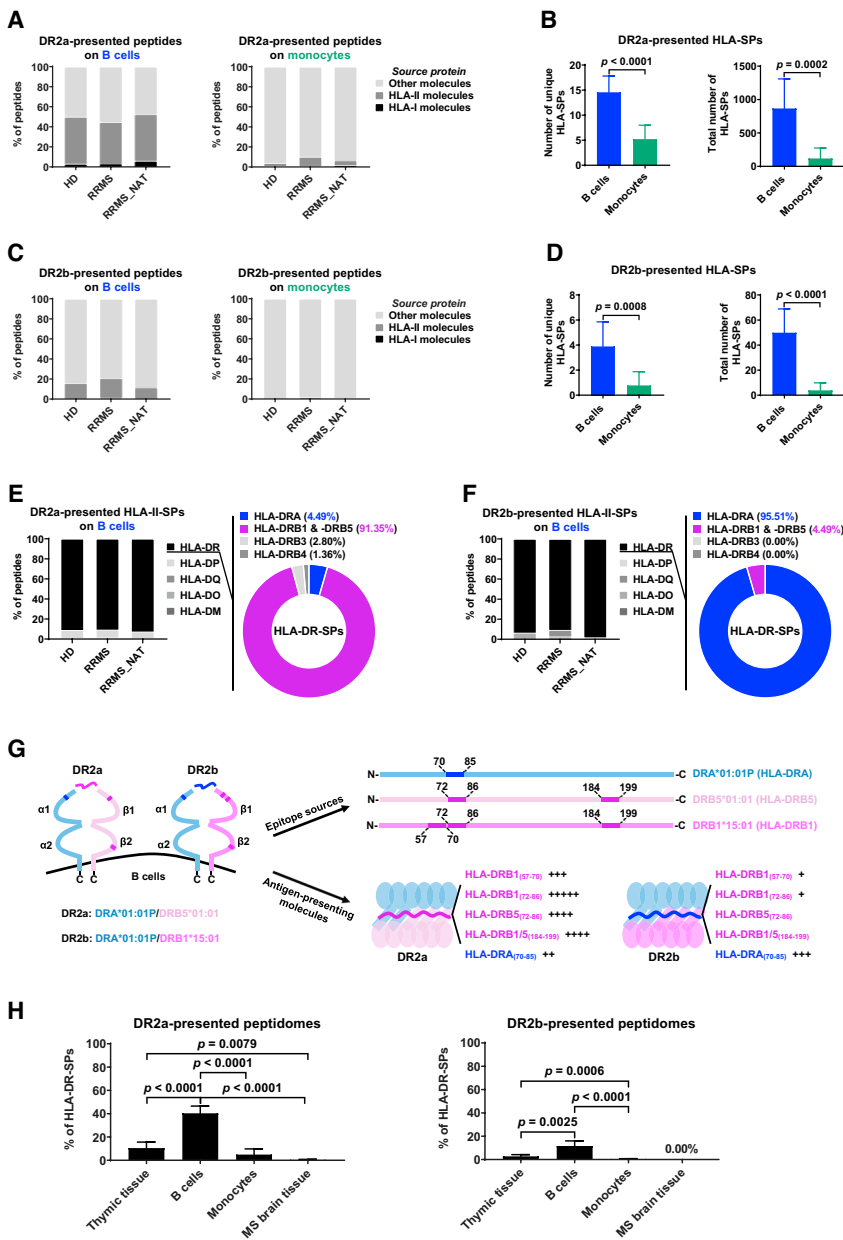
Figure 2. DR2a and DR2b Present Higher Numbers of HLA-DR-SPs on Primary B Cells Compared to Monocytes

(A) Frequencies of HLA-SPs in the DR2a-presented immunopeptidomes on B cells and monocytes.

(B) Numbers of unique and total HLA-SPs presented by DR2a on B cells and monocytes. Statistical analyses include data from HDs, RRMS, and RRMS_NAT.

(C) Frequencies of HLA-SPs in the DR2b-presented immunopeptidomes on B cells and monocytes.

(D) Numbers of unique and total HLA-SPs presented by DR2b on B cells and monocytes. Statistical analyses include data from HDs, RRMS, and RRMS_NAT.

(E and F) Analyses of HLA-II-SPs regarding their origin from different HLA-II molecules (left panel) and HLA-DR-SPs regarding their origin from different HLA-DR molecules (right panel) presented by DR2a (E) or DR2b (F) on B cells.

(G) Graphical depiction how DR2a and DR2b serve as antigen-presenting molecules and epitope sources on peripheral blood B cells. The depicted peptides are representative of the five most prominent HLA-DR-SPs. The + symbol semiquantitatively indicates the number of each peptide with different length versions.

(H) Frequencies of the five most prominent HLA-DR-SPs in the DR2a- and DR2b-presented immunopeptidomes of thymic tissue (n = 4), primary B cells (n = 9), primary monocytes (n = 9), and MS brain tissue (n = 4). Statistical analyses of B cells and monocytes include data from HDs, RRMS, and RRMS_NAT.

Data are expressed as mean ± SEM, and p values were determined by unpaired t test. See also Figure S3 and Tables S2, S3, and S4.

Responses to CEF II peptide pool and tetanus toxin peptides, $TT_{(830–844)}$ and $TT_{(947–967)}$, were not stronger in MS patients (Figures 3A and S4D), indicating that there is no general hyperreactivity in MS patients. The response patterns in MS patients were heterogeneous with respect to recognition of individual peptides (Figure S4E). Proliferation could be blocked by an anti-HLA-DR antibody (Ab) (Figure 3B), and CD4+ T cells divided strongest (Figure 3C), indicating that memory CD4+ T cells recognize HLA-DR-SPs in the context of DR molecules. In contrast, naive CD4+ T cells did not respond to HLA-DR-SPs (Figure 3D). Regarding functional responses, we detected interferon γ (IFN-γ) and less interleukin-17A (IL-17A) and IL-17F in the supernatants of CD45RA− cells and purified CD4+ T cells upon stimulation with HLA-DR-SPs (Figures 3E and 3F), indicating that HLA-DR-SP-specific T cells possess a Th1 or polyfunctional Th1* phenotype. These data and expression of CCR6 and CXCR3 (Figure 3G), two chemokine receptors involved in brain homing (Balashov et al., 1999; Reboldi et al., 2009), are consistent with the phenotype of autoproliferating CD4+ T cells (Jelcic et al., 2018). Thus, HLA-DR-SPs may promote proliferation, migration, and secretion of pro-inflammatory cytokines of memory CD4+ cells in DR15+ MS patients upon TCR-peptide/DR contact.

DR2a and DR2b Present HLA-DR-SPs to Autoreactive CD4+ T Cells

We next asked whether DR2a and DR2b contributed to CD4+ T cell responses against HLA-DR-SPs. For this purpose, we employed APCs expressing a single DR heterodimer, a bare lymphocyte syndrome (BLS) B cell line lacking HLA-II expression, that was transfected with DRA and DRB1*15:01 (BLS-DR2b cells) or DRB5*01:01 (BLS-DR2a cells). Purified blood CD4+ T cells from DR15+ MS patients were co-cultured with
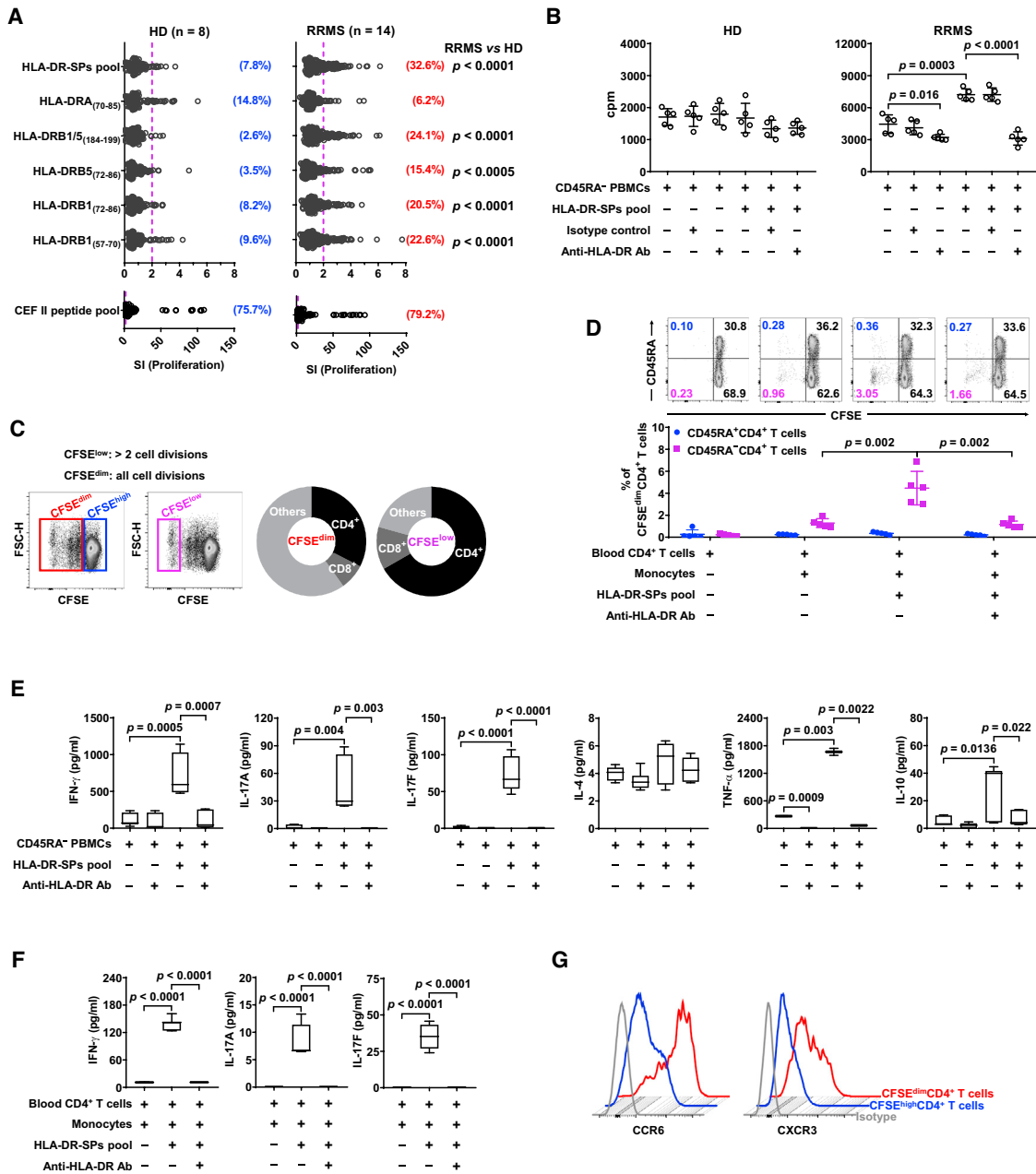
Figure 3. Increased Reactivity of Memory CD4+ T Cells against HLA-DR-SPs in MS Patients

(A) Responses of CD45RA⁻ PBMCs of HLA-DR15+ HDs (n = 8) and MS patients (RRMS, n = 4; RRMS_NAT, n = 10) against the five most common HLA-DR-SPs alone or as pool. 10–15 replicate wells were tested for proliferation, and responses are depicted as the stimulatory index (SI). Individual wells are represented by dots for HDs (left) or MS patients (right). The purple dotted line indicates SI = 2, and SI ≥ 2 was considered positive. Responses to control CEF II peptides are shown at the bottom.

(B) Proliferations of CD45RA⁻ PBMCs from HDs and MS patients after stimulation with pooled HLA-DR-SPs in the presence of a blocking anti-HLA-DR Ab.

(C) CD45RA⁻ PBMCs from HLA-DR15+ MS patients were labeled with carboxyfluorescein succinimidyl ester (CFSE) and stimulated with pooled HLA-DR-SPs. After 7 days, cells were analyzed, and proportions of memory CD4+ T cells in the proliferating (CFSE^dim) and highly proliferating (CFSE^low) compartments are shown in the pie charts.

(D) Blood CD4+ T cells and monocytes were purified from PBMCs of HLA-DR15+ MS patients and co-cultured with pooled HLA-DR-SPs for 7 days. Proliferation of naive CD4+ T cells (CD45RA+) and memory CD4+ T cells (CD45RA⁻) was detected.

(E) Th1/Th2/Th17-related cytokines in supernatants of CD45RA⁻ PBMCs after stimulation with pooled HLA-DR-SPs.

(F) IFN-γ, IL-17A, and IL-17F in supernatants of co-cultured blood CD4+ T cells and monocytes after stimulation with pooled HLA-DR-SPs.

(G) Expression levels of CCR6 and CXCR3 on non-proliferating (CFSE^high) and proliferating (CFSE^dim) memory CD4+ T cells after stimulation with pooled HLA-DR-SPs for 7 days.

Data are expressed as mean ± SEM, and p values were determined by unpaired t test. See also Figure S4 and Tables S1 and S5.

irradiated BLS-DR2a or BLS-DR2b cells and stimulated with HLA-DR-SPs. HLA-DR-SPs activated memory CD4$^+$ T cells when presented by DR2a and DR2b, and proliferation could be blocked by the anti-HLA-DR Ab. Very few CD45RA$^+$ naive CD4$^+$ T cells responded (Figure 4A). IFN-γ was detected in supernatants when BLS-DR2a and BLS-DR2b cells were used as APCs (Figure 4B). Thus, DR2a and DR2b can promote proliferation of memory CD4$^+$ T cells in DR15$^+$ MS patients by presenting HLA-DR-SPs.

To explore the potential role of HLA-DR-SP-specific memory CD4$^+$ T cells in MS, we first stimulated cerebrospinal fluid (CSF)-infiltrating CD4$^+$ T cells from DR15$^+$ MS patients (Table S6) with HLA-DR-SPs, assuming that T cells from the CNS compartment were more likely to be associated with MS. CSF-infiltrating CD4$^+$ T cells in 2 of 9 MS patients responded to HLA-DR-SPs presented by DR2a and 4 of 9 when presented by DR2b (Figure 4C). Thus, CD4$^+$ T cells recognizing HLA-DR-SPs in the context of both DR15 allomorphs can be found in the CSF in a substantial fraction of patients. Because very few or no HLA-DR-SPs could be found in the immunopeptidomes of brain APCs (Figure 2H), HLA-DR-SPs are likely not involved in intra-parenchymal re-stimulation or direct brain damage by autoreactive CD4$^+$ T cells.

We next addressed whether HLA-DR-SP-responsive CD4$^+$ T cells recognized putative MS autoantigens by stimulating CD45RA$^-$ PBMCs of MS patients with pooled HLA-DR-SPs and generating HLA-DR-SP-specific T cell lines (Figures S5A and S5B; Table S1). Testing with myelin peptide pools and known individual peptides that are targets of high-avidity CD4$^+$ T cells in MS, brain-infiltrating CD4$^+$ T cells in MS, or encephalitogenic in animals (Bielekova et al., 2004; Jelcic et al., 2018; Planas et al., 2018) demonstrated that HLA-DR-SP-specific CD4$^+$ T cells recognized these autoantigens on DR2a and DR2b (Figures 4D and S5B). Among the recognized individual peptides, myelin basic protein (MBP) peptide MBP$_{(83-99)}$ was also represented in MBP pool 3 and RASGRP2$_{(78-87)}$ in RASGRP2 pool 2 (Figures 4D and S5B). To further examine this aspect, we tested whether MBP$_{(83-99)}$-specific and RASGRP2$_{(78-87)}$-specific autoreactive T cell clones (TCCs) recognized HLA-DR-SPs. We selected the three well-characterized autoreactive CD4$^+$ TCCs TCC3A6, TCC5F6, and TCC14, all from DR15$^+$ MS patients. When testing these TCCs with individual and pooled HLA-DR-SPs, MBP$_{(83-99)}$-specific TCC3A6 and TCC5F6 did not respond to HLA-DR-SPs, whereas RASGRP2$_{(78-87)}$-specific TCC14 recognized DRB1$_{(57-70)}$, DRB1/5$_{(184-199)}$, and the HLA-DR-SPs pool (Figure 4E) and produced Th2 cytokines (Figure 4F). However, the stimulatory strength of DRB1$_{(57-70)}$ and DRB1/5$_{(184-199)}$ was much lower than that of RASGRP2$_{(78-87)}$ (Figures 4E and 4F). Responses to DRB1$_{(57-70)}$ and DRB1/5$_{(184-199)}$ could be blocked by the anti-HLA-DR Ab (Figure 4G), indicating that they are presented by DR2b.

These results indicate that DR2a and DR2b as well as their presented HLA-DR-SPs may participate in MS pathogenesis by activation and/or maintenance of autoreactive CD4$^+$ T cells through cross-reactivity.

HLA-DR-SPs Maintain Autoreactive CD4$^+$ T Cells in MS Patients

Dose titration of RASGRP2$_{(78-87)}$ and the two HLA-DR-SPs showed that TCC14 recognized RASGRP2$_{(78-87)}$ with high func-

tional avidity (EC$_{50}$ = 0.015 μM), but DRB1$_{(57-70)}$ and DRB1/5$_{(184-199)}$ with much lower avidity (Figure 5A). Expression of the activation markers CD69 and CD25 further supported this notion (Figure 5B). DRB1$_{(57-70)}$ and DRB1/5$_{(184-199)}$ are therefore weak or partial agonists, whereas the potentially "pathogenic" SP RASGRP2$_{(78-87)}$ is a strong agonist. Thus, DRB1$_{(57-70)}$ and DRB1/5$_{(184-199)}$ might be involved in peripheral maintenance but not full activation of TCC14.

We next addressed whether the above observations with a single RASGRP2$_{(78-87)}$-specific TCC also held for other MS patients by stimulating CD45RA$^-$ PBMCs from 3 RRMS_NAT patients with RASGRP2$_{(78-87)}$ to generate specific TCCs (Table S1). We chose RRMS_NAT patients based on previous data showing that autoreactive T cells are enriched in peripheral blood because of the inhibition of migration to the brain/CSF (Jelcic et al., 2018). Memory CD4$^+$ T cells from RRMS_NAT-1 and RRMS_NAT-2 responded to RASGRP2$_{(78-87)}$ (Figure 5C), and new RASGRP2$_{(78-87)}$-specific TCCs were isolated from both (Figure 5D). Multiple TCCs from RRMS_NAT-2 responded to RASGRP2$_{(78-87)}$ and DRB1$_{(57-70)}$ (Figure 5D), consistent with the marked proliferation of CD45RA$^-$ PBMCs from this patient to DRB1$_{(57-70)}$ (Figure S4E). Five of the new CD4$^+$ TCCs, 1159AG_TCC1–TCC5, reacting to RASGRP2$_{(78-87)}$ and DRB1$_{(57-70)}$, were identified (Figure 5E). All were DR2b restricted (Figure 5F) but different from TCC14, displayed a Th1/Th1* phenotype (Figure 5E), and secreted IFN-γ upon stimulation with RASGRP2$_{(78-87)}$ (Figure 5G). Testing 1159AG_TCCs against another HLA-DR-SP that TCC14 recognized, DRB1/5$_{(184-199)}$, showed that only 1159AG_TCC3 responded with proliferation (Figure 5H) but 4 of 5 with IFN-γ secretion (Figure 5I). Importantly, like TCC14, reactivity to DRB1$_{(57-70)}$ and DRB1/5$_{(184-199)}$ was weaker than against RASGRP2$_{(78-87)}$ for all 1159AG_TCCs (Figures 5D, 5H, and 5I). Thus, cross-reactivity between HLA-DR-SPs and RASGRP2 is frequent in MS patients, and the main role of HLA-DR-SPs is likely in homeostatic maintenance of autoreactive memory CD4$^+$ T cells in DR15$^+$ MS patients by low-avidity interactions between TCR and HLA-DR-SP/DR complexes on B cells.

The above findings led us to ask why RASGRP2-specific CD4$^+$ T cells could be identified relatively easily in DR15$^+$ MS patients. Immunodominance of peptides and a higher frequency of autoreactive T cells with specificity for peptides of myelin oligodendrocyte glycoprotein (MOG), proteolipid protein (PLP), or MBP have been linked to the absence of thymic expression (Bruno et al., 2002; Klein et al., 2000) or low DR binding affinity (Muraro et al., 1997). Regarding RASGRP2, we analyzed its gene expression in thymic epithelial cells (TECs) from DR15$^+$ individuals; i.e., the cells that mediate negative selection to remove high-avidity autoreactive T cells and establish central tolerance (Klein et al., 2014). Similar to MOG and PLP (Bruno et al., 2002; Klein et al., 2000, 2014), RASGRP2 expression was absent or at the detection threshold in TECs (Figure S5C), explaining how RASGRP2-specific autoreactive CD4$^+$ T cells could escape negative selection and be found relatively frequently in the periphery.

Different from RASGRP2, DRA, DRB1, and DRB5 were highly expressed in TECs (Figure S5D), and HLA-DR-SPs were present in the DR2a and DR2b immunopeptidomes from DR15$^+$ thymic
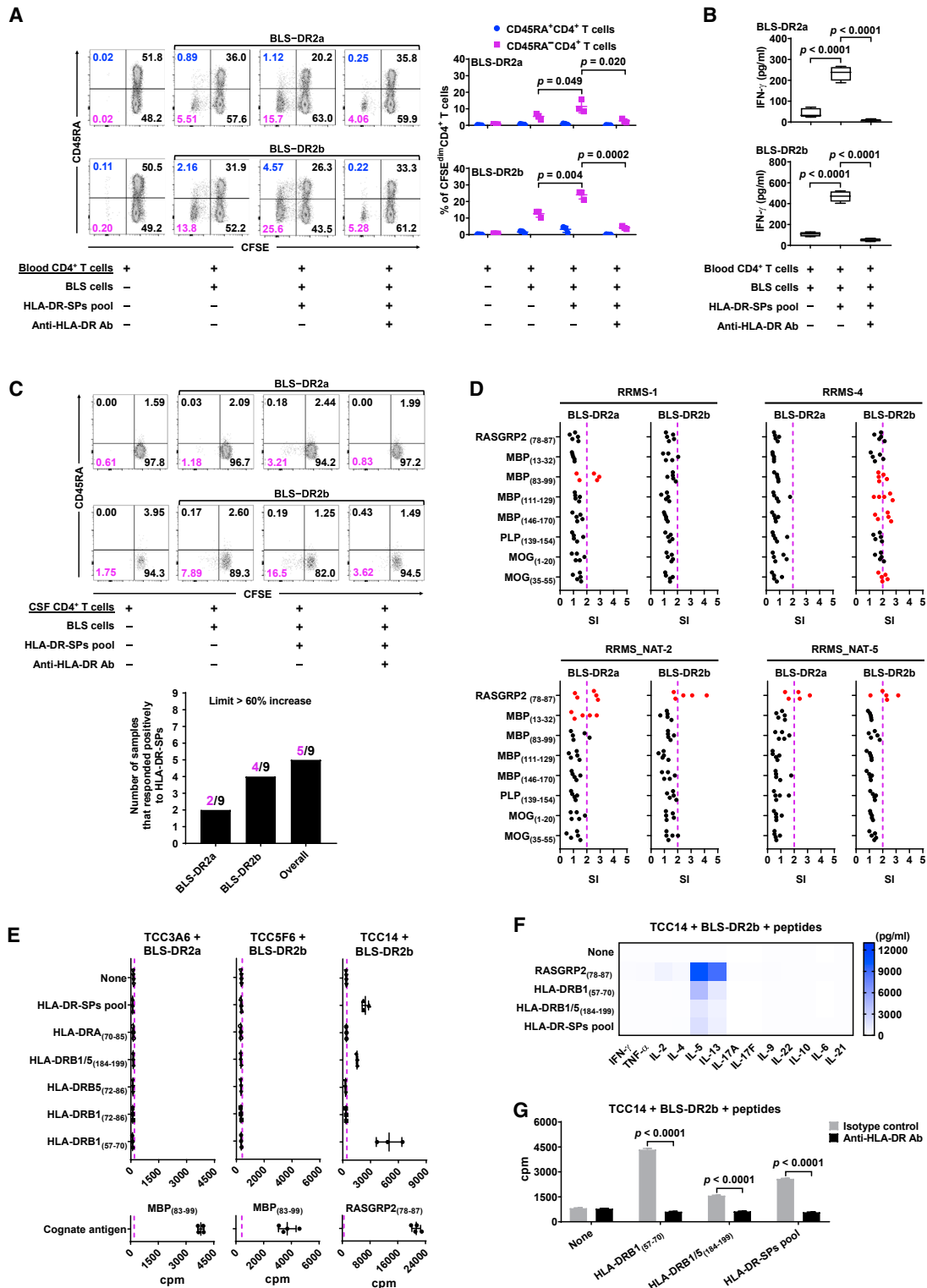
Figure 4. DR2a and DR2b Present HLA-DR-SPs to Autoreactive CD4+ T Cells

(A and B) Purified blood CD4+ T cells of HLA-DR15+ MS patients were co-cultured with irradiated BLS-DR2a or BLS-DR2b cells as APCs and stimulated with pooled HLA-DR-SPs for 7 days. Shown is proliferation of naive (CD45RA+) and memory (CD45RA−) CD4+ T cells (A) and IFN-γ in supernatants (B).
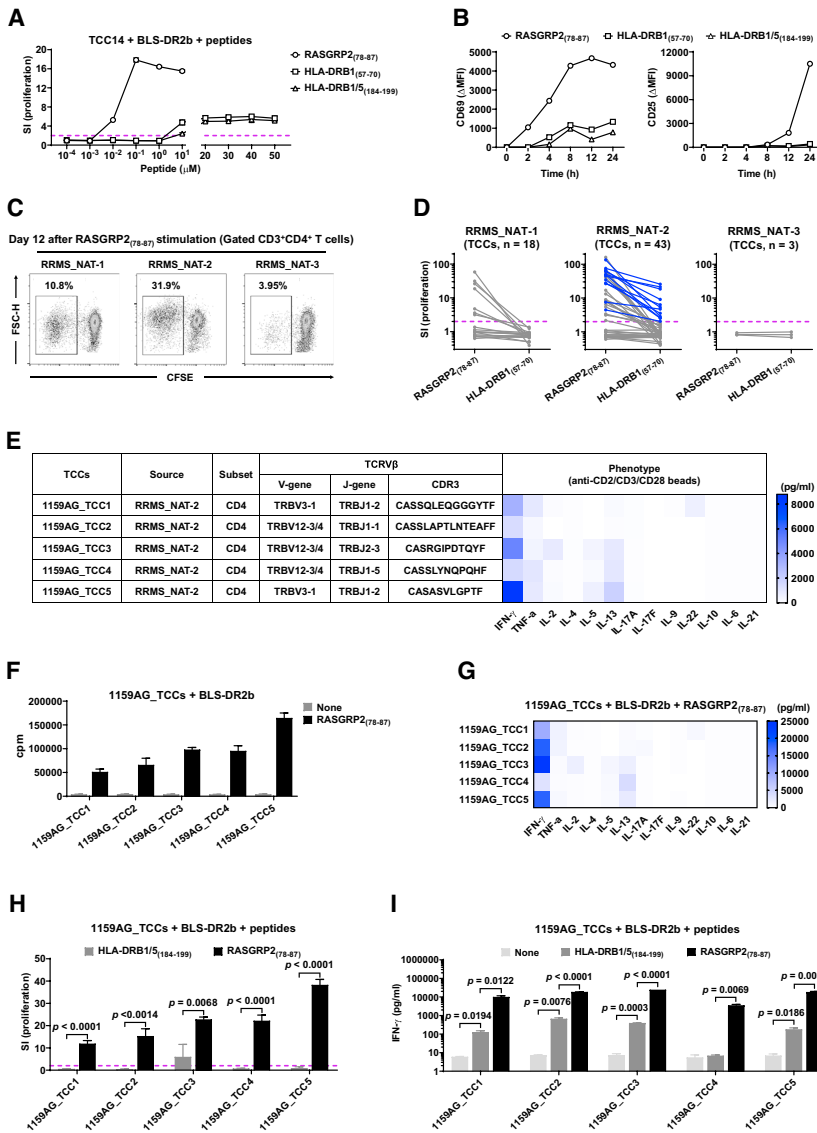
(legend continued on next page)

Figure 5. Responses of Autoreactive CD4+ TCCs to RASGRP2 and HLA-DR-SPs

(A) Dose-response curves of TCC14 to RASGRP2$_{(78-87)}$ and HLA-DR-SPs.

(B) Irradiated BLS-DR2b cells were incubated with peptides for 12 h and then co-cultured with TCC14. Shown are expression levels of CD69 and CD25 on TCC14 at different time points after co-culture. ΔMFI indicates the mean fluorescence intensity (MFI) value above the no-peptide control.

(C–E) CD45RA− PBMCs from 3 HLA-DR15+ RRMS_NAT patients were stimulated with RASGRP2$_{(78-87)}$ to generate TCCs. Proliferation of memory CD4+ T cells was analyzed on day 12 (C). Acquired TCCs were co-cultured with irradiated autologous PBMCs as APCs and stimulated with RASGRP2$_{(78-87)}$ or DRB1$_{(57-70)}$, and proliferation was detected on day 3. The TCCs responding to RASGRP2$_{(78-87)}$ and DRB1$_{(57-70)}$ are highlighted in blue (D). Five new 1159AG_TCCs that responded to RASGRP2$_{(78-87)}$ and DRB1$_{(57-70)}$ were generated from RRMS_NAT-2. Their corresponding TCRVβ sequence and functional phenotype are shown (E).

(F) Restriction of the RASGRP2$_{(78-87)}$-specific 1159AG_TCCs was tested with irradiated BLS-DR2b cells and stimulation with RASGRP2$_{(78-87)}$.

(G) Th1/Th2/Th17-related cytokines in supernatants of 1159AG_TCCs after co-culture with irradiated BLS-DR2b cells and stimulation with RASGRP2$_{(78-87)}$ for 3 days.

(H and I) 1159AG_TCCs were co-cultured with irradiated BLS-DR2b cells and stimulated with RASGRP2$_{(78-87)}$ or DRB1/5$_{(184-199)}$ for 3 days. Shown is proliferation of 1159AG_TCCs (H) and IFN-γ in supernatants (I).

Data are expressed as mean ± SEM, and p values were determined by unpaired t test. See also Figures S4 and S5 and Table S1.

tissues (Figure 2H). Although not formally shown for thymocytes, high-avidity RASGRP2-specific CD4+ T cells, which cross-reacted to HLA-DR-SPs with much lower avidity, might be positively selected in the thymus and subsequently be maintained in the periphery by the latter. This had been speculated after the first demonstration that MHC-SPs are part of the MHC class II-presented immunopeptidome (Baum et al., 1995b; Kourilsky and Claverie, 1989).

(C) CSF-infiltrating CD4+ T cells of HLA-DR15+ MS patients (n = 9) were co-cultured with irradiated BLS-DR2a or BLS-DR2b cells and stimulated with pooled HLA-DR-SPs for 7 days. Proliferation of CSF-infiltrating CD4+ T cells is shown. The bar graph at the bottom indicates the number of donors responding to the pooled HLA-DR-SPs. Increases of more than 60% above controls were considered positive.

(D) Proliferation of HLA-DR-SP-specific bulk CD4+ T cells from HLA-DR15+ MS patients (n = 4) after co-culture with irradiated BLS-DR2a or BLS-DR2b cells and stimulation with the putative MS target antigens RASGRP2$_{(78-87)}$, MBP$_{(13-32)}$, MBP$_{(83-99)}$, MBP$_{(111-129)}$, MBP$_{(146-170)}$, PLP$_{(139-154)}$, MOG$_{(1-20)}$, and MOG$_{(35-55)}$ for 7 days (5 replicate wells). Groups with 2 or more positive wells are highlighted in red.

(E) Proliferations of autoreactive TCC3A6, TCC5F6, or TCC14 after co-culture with irradiated BLS-DR2a or BLS-DR2b cells and stimulation with HLA-DR-SPs for 3 days. Responses to the cognate autoantigen are shown at the bottom. The purple dotted line indicates the mean + 3SD of the no-peptide control, and values above the purple dotted line were considered positive.

(F) Th1/Th2/Th17-related cytokines in supernatants of TCC14 after co-culture with irradiated BLS-DR2b cells and stimulation with RASGRP2$_{(78-87)}$ or HLA-DR-SPs for 3 days.

(G) Proliferation of TCC14 after co-culture with irradiated BLS-DR2b cells and stimulation with HLA-DR-SPs for 3 days in the presence of anti-HLA-DR Ab.

Data are expressed as mean ± SEM, and p values were determined by unpaired t test. See also Figure S5 and Tables S1 and S6.

MS-Associated Foreign Antigens Trigger Autoreactive CD4+ T Cells by Cross-reactivity

HLA-DR-SPs can be viewed as "selecting/homeostatic" SPs that can participate in thymic selection and/or homeostatic maintenance of potentially autoreactive CD4+ T cells. However, their full activation probably involves stronger ligands; e.g., peptides from foreign agents. It is well known that the DR15 haplotype amplifies the effect of certain environmental risk factors for MS, most notably of altered immunity to EBV (Olsson et al., 2017). This effect may be mediated by molecular mimicry between peptides from EBV and SPs, which are presented by DR15 molecules and cross-recognized by autoreactive CD4+ T cells (Planas et al., 2018; Tengvall et al., 2019; Wucherpfennig and Strominger, 1995). To address this point, we chose EBV and another pathogen implicated in MS, a bacterial taxon overrepresented in gut microbiota of MS patients, *Akkermansia muciniphila* (Berer et al., 2017; Cekanaviciute et al., 2017; Jangi et al., 2016). We used data from testing TCC14 with combinatorial peptides libraries and a dedicated biometrical analysis (Zhao et al., 2001) to predict potentially stimulatory peptides from EBV and *Akkermansia* (Figure S6A). The scores of all decapeptides from both agents ranged between 20 and 125, well below the theoretical maximum score of 190.88 for TCC14 (Figure S6B). Previous studies had shown a positive relationship between peptides with predicted high scores and T cell responses (Sospedra et al., 2010). We therefore selected peptides from EBV (n = 33) and *Akkermansia* (n = 30) with scores between 75 and 125 (Figure S6B; Table S7), synthesized and tested them with TCC14. Indeed, two EBV and nine *Akkermansia* peptides gave positive responses (Figure 6A). As controls, we chose a herpesvirus negatively associated with MS, human cytomegalovirus (HCMV) (Sundqvist et al., 2014), and a bacterium considered protective for MS, *Prevotella histicola* (Shahi et al., 2019), and again selected peptides with scores of 75–125 (Figure S6C; Table S7). TCC14 did not react to any peptide from these two agents (Figure 6B). Compared with DRB1$_{(57–70)}$ and DRB1/5$_{(184–199)}$, two EBV and four *Akkermansia* peptides exhibited stronger effects (Figure 6A). Further, some peptides from EBV and *Akkermansia* activated TCC14 comparably with RASGRP2$_{(78–87)}$, based on upregulation of CD69 and CD25, downregulation of surface TCR (Figure 6C), and production of Th2 cytokines (Figure 6D). To address the stimulatory hierarchy in more detail, we performed transcriptional profiling by RNA sequencing and found that the up- and downregulation of a broad range of genes corresponded to the stimulatory strength of the peptides (Figure 6E). Regarding the rank order of broad sets of genes related to activation, proliferation, and Th2 function, EBV and *Akkermansia* peptides were stronger than HLA-DR-SPs and close to RASGRP2$_{(78–87)}$ (Figure 6F). However, the upregulation of genes related to cytotoxicity and/or pathogenesis of MS and experimental autoimmune encephalomyelitis (EAE), including GZMB (Granzyme B), FASLG (Fas ligand), CSF2 (granulocyte-macrophage colony-stimulating factor [GM-CSF]), and IL-3, was more pronounced with RASGRP2$_{(78–87)}$ compared with EBV and *Akkermansia* peptides (Figure 6F). Moreover, when testing 1159AG_TCCs with peptides that had been selected from foreign agents for TCC14, two *Akkermansia* peptides also stimulated proliferation (Figure 6G) and IFN-γ pro-

duction (Figures 6H, S6D, and S6E), whereas all peptides from HCMV and *Prevotella* were negative (Figures S6F and S6G). These data suggest that the MS-associated foreign agents EBV and *Akkermansia* might be involved in activation/expansion of autoreactive memory CD4+ T cells via molecular mimicry.

Cross-restriction of Autoreactive CD4+ T Cells by DR2a and DR2b

Besides T cell cross-reactivity, others and we have shown that the same and/or different peptides can be recognized by a single TCR in the context of several HLA-II molecules, including DR2a and DR2b (Lang et al., 2002; Yousef et al., 2012; Figures 7A and S7). We referred to this characteristic as HLA cross-restriction and wanted to find out whether an autoreactive CD4+ T cell recognized the above peptides in the context of both DR15 allomorphs. Indeed, TCC14 reacted to RASGRP2$_{(78–87)}$ presented by DR2a and DR2b and maintained its Th2 phenotype, although the response to RASGRP2$_{(78–87)}$/DR2a was lower (Figures 7B and 7C). Further, transcriptome analysis indicated that TCC14 responded to RASGRP2$_{(78–87)}$ presented by DR2a and DR2b in a similar manner, although restriction by DR2b was always more efficient (Figures 7D and 7E). Like TCC14, the DR2b-restricted 1159AG_TCC2, 1159AG_TCC3, and 1159AG_TCC5 also reacted to RASGRP2$_{(78–87)}$ presented by DR2a (Figure 7F) and maintained their Th1/Th1* phenotype (Figure 7G). In addition to RASGRP2$_{(78–87)}$, one EBV and three *Akkermansia* peptides activated TCC14 together with DR2a (Figure 7H), but less strongly than RASGRP2$_{(78–87)}$ (Figure 7I). These data demonstrate another facet of the cooperative effects of the two MS-associated DR15 allomorphs that extends beyond serving as antigen-presenting molecule and epitope source. It appears that the structures of DR2a and DR2b after binding foreign peptides from EBV and *Akkermansia* or autoantigenic peptide from RASGRP2 are sufficiently similar to activate a TCC like TCC14.

DISCUSSION

The HLA gene complex, one of the most polymorphic regions of the genome, has evolved under the pressure of pathogens, and the high prevalence of certain HLA molecules in populations of distinct geographic areas and ethnicity is explained by this interplay (Blackwell et al., 2009). As a downside, fitness to cope with dangerous pathogens in the context of certain HLA molecules comes at the price of misguided immune responses. In the field of HLA genotyping, it has long been known that DRB1*15:01 and DRB5*01:01 are found to be virtually 100% linked in Caucasoids, the ethnic group with the highest MS prevalence (Tiercy et al., 1991). We further confirm this here for over 500 northern European DR15+ MS patients. Despite this knowledge, one striking aspect of MS genetics research has been its focus on DRB1*15:01/DR2b, with a recent study being most representative (Moutsianas et al., 2015), whereas only few examined DRB5*01:01/DR2a (Caillier et al., 2008; Gregersen et al., 2006; Martin et al., 1991; Pette et al., 1990; Wucherpfennig et al., 1994). This is in part due to the fact that common variants are spaced sufficiently tightly to assign DRB1* but not DRB3*, DRB4* and DRB5* genes (Dilthey et al., 2011).
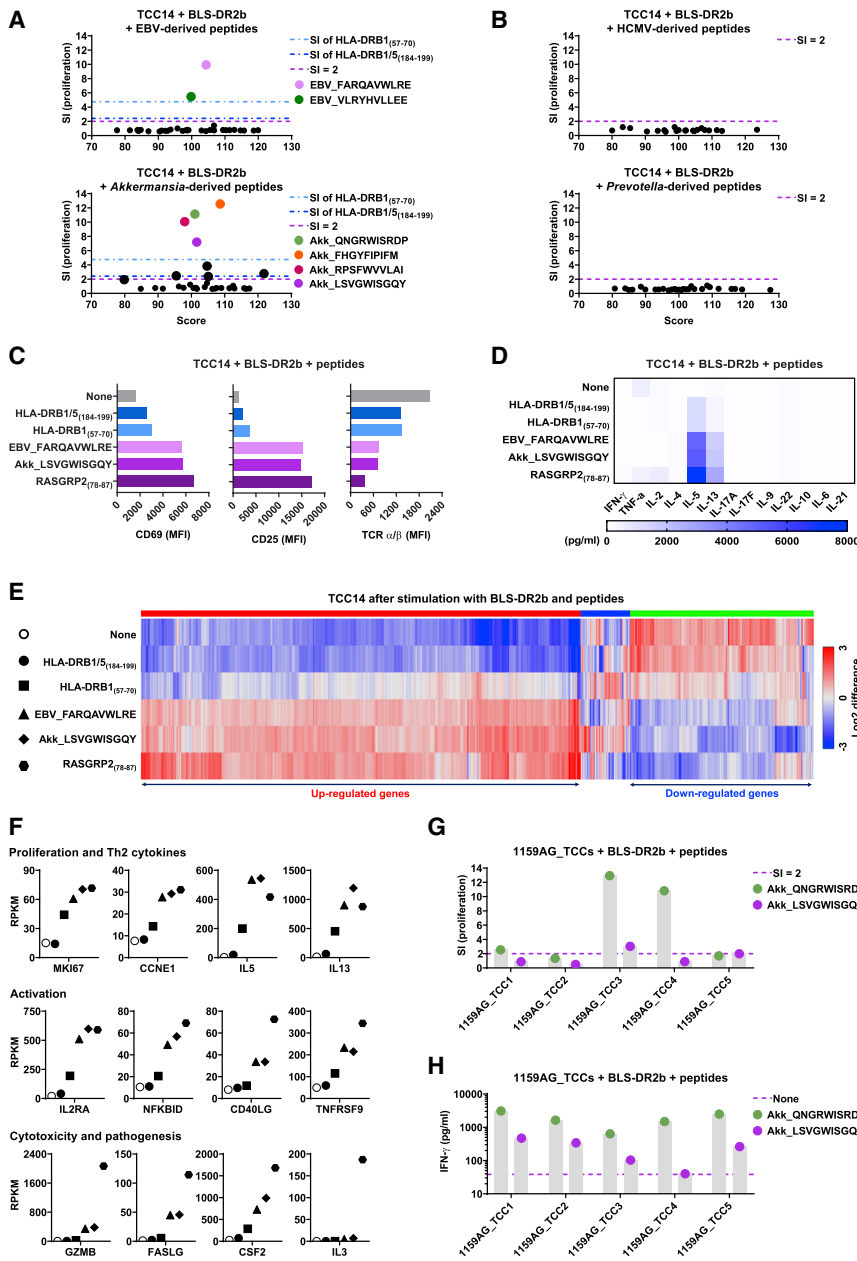
Figure 6. RASGRP2-Specific CD4$^+$ T Cells Are Activated by Peptides from MS-Associated Foreign Agents

(A and B) TCC14 was tested with predicted stimulatory decapeptides from the MS-associated pathogens EBV and *Akkermansia* (A) and control peptides from HCMV and *Prevotella* (B). Proliferation was detected on day 3. The x axis indicates the predicted stimulatory score of each peptide using the scoring matrix in Figure S6A.

(C and D) Irradiated BLS-DR2b cells were incubated with peptides for 12 h and then co-cultured with TCC14 for 24 h. Shown are upregulation of CD69 and CD25 and downregulation of TCR α/β on TCC14 (C) and Th1/Th2/Th17-related cytokines in supernatants (D).

(E) Heatmap showing the top 1,000 high-variant genes that increased or decreased expression in TCC14 after co-culture with irradiated BLS-DR2b cells and stimulation with HLA-DR-SPs, peptides from EBV and *Akkermansia*, and RASGRP2$_{(78-87)}$ for 24 h.

(F) Expression levels of genes related to proliferation and Th2 cytokines (MKI67 [Ki-67], CCNE1 [Cyclin E1], IL-5, and IL-13), T cell activation (IL2RA [CD25], NFKBID [nuclear factor κB (NF-κB) inhibitor delta], CD40LG [CD40 ligand], and TNFRSF9 [4-1BB]) as well as cytotoxicity and MS pathogenesis (GZMB, FASLG, CSF2, and IL-3) in TCC14 after co-culture with irradiated BLS-DR2b cells and stimulation with HLA-DR-SPs, peptides from EBV and *Akkermansia*, and RASGRP2$_{(78-87)}$ for 24 h. The mRNA expression levels are expressed as RPKM (reads per kilobase per million mapped reads).

(G and H) 1159AG_TCCs were tested with predicted stimulatory decapeptides from EBV and *Akkermansia*. Proliferation was detected on day 3. Two positive peptides from *Akkermansia* are shown (G), as well as IFN-γ in supernatants (H).

Data are expressed as mean or mean ± SEM. See also Figure S6 and Table S7.

Regarding the functional role of DR2a, one study has shown protective effects of DRB5*01:01 in humanized transgenic mice in which co-expression of DR2a lowers the disease susceptibility conferred by DRB1*15:01 (Gregersen et al., 2006). Another noted faster conversion to progressive MS in African-American MS patients who expressed DRB1*15:03 and no DRB5*01:01, indicating that the latter is not required for MS (Caillier et al., 2008). But our own data, including (1) spontaneous EAE in humanized transgenic mice expressing an MS patient-derived, MBP-specific TCR and DRB5*01:01(Quandt et al., 2012); (2) the pro-inflammatory phenotype of DR2a-restricted myelin-specific TCC (Hemmer et al., 1997); (3) the higher DR2a expression on several APCs and in the brain (Prat et al., 2005);

and (4) similarities of peptide binding motifs of the two DR15 allomorphs (Southwood et al., 1998; Vogt et al., 1994; Wucherpfennig et al., 1994) argue that DR2a should be considered an MS-associated genetic risk factor. Whether SNPs in the DRB5*01:01 gene are related to differential methylation and DR expression, as has been shown for DRB1*15:01, should be considered in the future (Kular et al., 2018).

We analyzed the immunopeptidomes of both DR15 allomorphs on primary B cells, an APC type, which a number of indirect approaches identified as important for MS pathogenesis (Hauser et al., 2008; Jelcic et al., 2018; Li et al., 2015; Molnarfi et al., 2013; Sabatino et al., 2019). Different from prior studies of immunopeptidomes from EBV-transformed B cell lines, BLS-DR2a or BLS-DR2b cells (Scholz et al., 2017; Vogt et al., 1994) and for other DR molecules (Chicz et al., 1992, 1993; Rudensky et al., 1991), we examined primary B cells. The B cell- and monocyte-derived immunopeptidomes disclosed similar
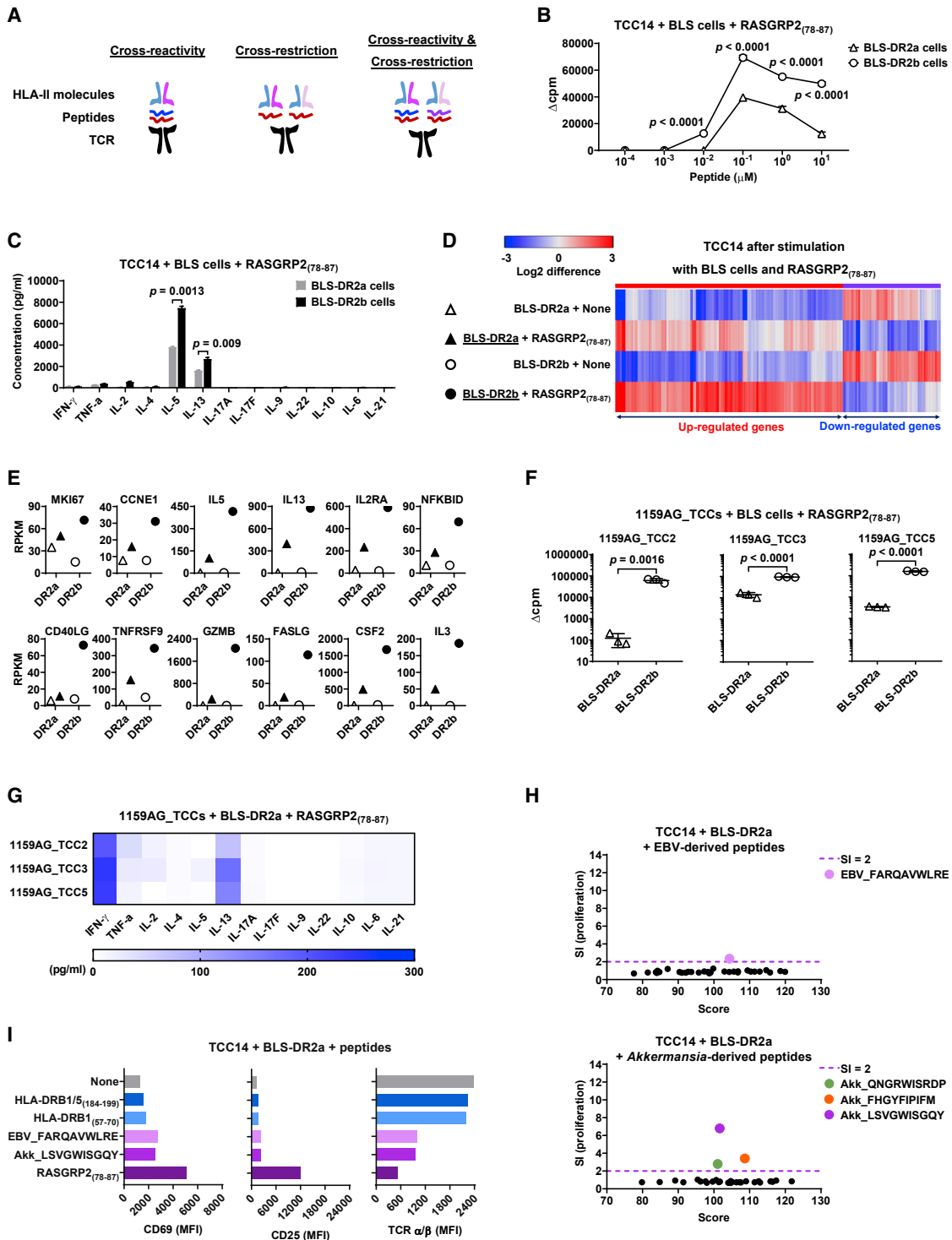
Figure 7. Cross-restriction in Recognizing RASGRP2$_{(78–87)}$ in the Context of DR2a and DR2b

(A) Graphical depiction of TCR cross-reactivity (left; that is, recognition of two or more peptides by a single TCR in the context of one HLA-restriction element [e.g., DR2a or DR2b]), HLA cross-restriction (center; that is, recognition of the same or different peptides by a single TCR in the context of several HLA-II molecules [here DR2a and DR2b]), and the combination of cross-reactivity and HLA cross-restriction (right).

(B) Dose-response curves of TCC14 to RASGRP2$_{(78–87)}$ using irradiated BLS-DR2a or BLS-DR2b cells as APCs. Proliferation was detected on day 3. Δcpm indicates the counts per minute value above the no-peptide control.

(legend continued on next page)

binding motifs as prior data (Vogt et al., 1994), but B cell-derived peptides differed from monocytes in that 20%–50% of peptides presented by DR2a and DR2b on B cells originated from HLA-II molecules and almost exclusively from DR2a and DR2b themselves, although they were also found on monocytes. HLA-I-SPs and HLA-II-SPs have been shown previously in the DR2a/DR2b-presented immunopeptidomes (Mohme et al., 2013; Scholz et al., 2017; Vogt et al., 1994), but their high prevalence on primary B cells was not known. Also, that most peptides on DR2a stemmed from the DR β chain whereas those on DR2b originated primarily from the DR α chain is novel. A few peptides, albeit with varying lengths, thus occupied a considerable fraction of surface DR2a and DR2b on peripheral blood B cells. Thus, disease-associated DR15 molecules can serve as antigen-presenting structures and sources of epitopes. In one prior study, variations of three of the five HLA-DR-SPs had been eluted from DR molecules of dendritic cells (DCs)-depleted thymic APCs (Adamopoulou et al., 2013). The authors used a pan-HLA-DR Ab, and peptides could therefore not be assigned to one of the two DR15 allomorphs. Two of the five peptides could also be isolated from thymic DCs (Adamopoulou et al., 2013); therefore, some of the HLA-DR-SPs, which are abundant on peripheral blood B cells and thymic tissues, may act during CD4$^+$ T cell selection. We did not differentiate TECs, DC types, or thymic B cells (Klein et al., 2014) and therefore do not know how HLA-DR-SPs may contribute to positive and negative selection. Cortical TECs are most likely involved in positively selecting HLA-DR-SP-reactive T cells, whereas those with high avidity are probably deleted by negative selection (Klein et al., 2014). This is compatible with our observation that naive CD4$^+$ T cells did not respond to HLA-DR-SPs but were probably homeostatically maintained whereas memory CD4$^+$ T cells did.

Memory CD4$^+$ T cells downregulate their activation threshold after activation by high-avidity ligands (Stefanová et al., 2002), such as the peptides from the two MS-associated pathogens EBV and *Akkermansia*. Interestingly, the EBV-derived peptides are from the lytic viral gene products BHRF1 and BPLF1, which drive lymphocytosis during mononucleosis (Taylor et al., 2015), which strongly raises the risk to develop MS (Olsson et al., 2017). BHRF1- and BPLF1-specific CD4$^+$ T cells could be primed aberrantly during mononucleosis and confer risk for MS development. After differentiation into memory cells, we assume, but cannot show *in vivo*, that HLA-DR-SPs are involved in homeostatic maintenance of these CD4$^+$ T cells and also in au-

toproliferation (Jelcic et al., 2018; Mohme et al., 2013). Therefore, we considered HLA-DR-SPs as "selecting/homeostatic" SPs in the thymus and peripheral blood, respectively, where they might participate in shaping a TCR repertoire that confers protection against MS-associated foreign agents but can also potentially respond to pathogenic SPs from RASGRP2 or myelin, as shown for memory CD4$^+$ T cells, such as the brain-infiltrating TCC14, which recognized not only the putative MS autoantigen RASGRP2 (Jelcic et al., 2018) but also several HLA-DR-SPs and peptides derived from EBV and *Akkermansia*. Regarding the antigen hierarchy, HLA-DR-SPs are weak agonists, EBV and *Akkermansia* peptides are full agonists, and the RASGRP2 peptide is an even stronger ligand. High-avidity recognition of a potentially "pathogenic" SP like RASGRP2$_{(78-87)}$ fits with the absence of thymic transcription, as shown before for PLP (Klein et al., 2000) and MOG (Bruno et al., 2002).

At present, we do not know whether and under which conditions RASGRP2 expression might start *in vivo* in peripheral blood B cells or in the target organ brain. However, we assume that recognition of this peptide by naive CD4$^+$ T cells that had been selected by HLA-DR-SPs and converted to memory CD4$^+$ T cells by recognizing EBV or *Akkermansia* peptides may lead to their full activation in the periphery and/or the brain. This is not unique for TCC14 because we could easily isolate more pro-inflammatory TCCs with similar properties; i.e., cross-recognition of HLA-DR-SPs, RASGRP2, and *Akkermansia*. Our current data support that HLA-DR-SPs can be recognized as nominal antigens that share similarities with peptides from foreign antigens or potentially "pathogenic" SPs, but we cannot exclude that they may also act as co-agonists via integration in the immunological synapse (Krogsgaard et al., 2005) or that the specificity of TCR is determined by recognizing the backbone of the HLA molecules (Cai and Hafler, 2007). Also, how and whether recognition of the different peptides influences functional differentiation into specific Th subtypes (Adair et al., 2016) remains to be studied.

Assuming that both DR15 allomorphs jointly contribute to MS pathogenesis, it is curious that peptides from EBV and *Akkermansia* and from the potentially "pathogenic" RASGRP2 are recognized by TCC14 and additional clones in the context of both DR15 allomorphs. Others and we have previously observed HLA cross-restriction with brain-infiltrating John Cunningham (JC) polyomavirus-specific T cells (Yousef et al., 2012), with an MBP/EBV-specific CD4$^+$ TCC from a DR15$^+$ MS patient (Lang et al., 2002) and with CSF-infiltrating CD4$^+$ T cells in MS

(C) Th1/Th2/Th17-related cytokines in supernatants of TCC14 after co-culture with irradiated BLS-DR2a or BLS-DR2b cells and stimulation with RASGRP2$_{(78-87)}$ for 3 days.

(D) Heatmap showing a broad range of genes that increased or decreased expression in TCC14 after co-culture with irradiated BLS-DR2a or BLS-DR2b cells and stimulation with RASGRP2$_{(78-87)}$ for 24 h.

(E) Expression levels of the genes related to proliferation and Th2 cytokine, T cell activation, as well as cytotoxicity and MS pathogenesis in TCC14 after co-culture with irradiated BLS-DR2a or BLS-DR2b cells and stimulation with RASGRP2$_{(78-87)}$ for 24 h.

(F) Proliferation of 1159AG_TCCs after co-culture with irradiated BLS-DR2a or BLS-DR2b cells and stimulation with RASGRP2$_{(78-87)}$ for 3 days.

(G) Th1/Th2/Th17-related cytokines in supernatants of 1159AG_TCCs after co-culture with irradiated BLS-DR2a cells and stimulation with RASGRP2$_{(78-87)}$ for 3 days.

(H) Proliferation of TCC14 after co-culture with irradiated BLS-DR2a cells and stimulation with the predicted stimulatory decapeptides from EBV and *Akkermansia* for 3 days.

(I) Irradiated BLS-DR2a cells were incubated with the peptides for 12 h and then co-cultured with TCC14 for 24 h. Shown are upregulation of CD69 and CD25 and downregulation of TCR α/β on TCC14.

Data are expressed as mean ± SEM, and p values were determined by unpaired t test. See also Figure S7 and Table S7.

(Sospedra et al., 2006). HLA cross-restriction of CD4⁺ T cells contributes to controlling HIV (Galperin et al., 2018) and may also be critical for controlling viral infections in the brain, an immunoprivileged organ with low HLA-II expression (Yousef et al., 2012). The ability of a TCC to recognize cognate peptides on more than one HLA-II element may, however, also increase the risk of CNS damage by an autoreactive TCC. In the case of DR2a and DR2b, cross-restriction may involve similarities of the contact surfaces of the two molecules toward the TCR, whereas differences exist primarily in the peptide binding grooves (Li et al., 2000; Smith et al., 1998). Thus, the cooperation of DR2a and DR2b may increase the fitness to cope with viral infection but also the risk of pathogenic autoreactivity. A recent study documented that DR2a and DR2b are expressed highly in normal-appearing gray matter in MS brains (Enz et al., 2019), the region where RASGRP2 is found in cortical neurons (Jelcic et al., 2018).

Our data show the complexity of how the two MS-associated DR15 allomorphs could functionally contribute to MS as antigen-presenting structures and epitope sources during thymic selection and peripheral maintenance of a TCR repertoire. HLA-DR-SP-reactive CD4⁺ T cells could be activated by certain foreign agents like EBV and *Akkermansia* and then respond to potentially "pathogenic" SPs from RASGRP2 or autoantigens such as MBP in the blood and probably also the CSF/brain. At each step, DR2a and DR2b may serve as antigen-presenting structures, binding peptides from themselves, and be involved in cross-restriction. At present, we cannot provide solid evidence of every single step and in each compartment, particularly not in the selecting organ, the thymus, and the target, the brain. However, HLA-DR-SPs in the DR2a and DR2b immunopeptidomes in thymic tissues and peripheral blood B cells but not in the brain, activation of T cell responses against myelin and RASGRP2 by HLA-DR-SPs, and the recognition hierarchies of the HLA-DR-SPs versus EBV and *Akkermansia* peptides and RASGRP2 peptide are compatible with current concepts of T cell selection, peripheral maintenance, and full activation (Boyman et al., 2009; Takaba and Takayanagi, 2017).

In conclusion, DR2a and DR2b could jointly shape an autoreactive T cell repertoire in MS. Recognition of HLA-DR-SPs, potentially "pathogenic" SPs, and peptides from MS-associated pathogens demonstrates how the most important genetic risk factor may link immune reactivity to environmental risk factors and autoantigens at the level of TCR-peptide/DR recognition. The concepts of how HLA-SPs might be involved in molecular mimicry in autoimmune diseases like autoimmune hepatitis, RA, and T1D were formulated almost 30 years ago (Baum et al., 1995a, 1995b; Burroughs et al., 1992). Our experimental approaches outline how to address whether HLA-DR-SPs contribute to the strong associations between distinct HLA-DR molecules in a number of autoimmune diseases with clear HLA association, including RA, T1D, autoimmune thyroid disease, primary biliary cirrhosis, Goodpasture syndrome, narcolepsy, and others. The intriguing epidemiological and experimental data that exist for molecular mimicry between autoantigen and viral/bacterial pathogens in many of these diseases (Cusick et al., 2012) could be linked to T cell repertoire generation and maintenance by HLA-DR-SPs. Regarding therapeutic implications, blocking the T1D-associated HLA-DQ8 with the small

molecule methyldopa inhibits formation of anti-insulin Abs and spontaneous disease in animals (Ostrov et al., 2018). Another small molecule (PV-267) that fills the binding pocket of DR2b inhibits cytokine production and proliferation of DR2b-restricted, MBP-specific T cells and allows prevention and treatment in a DR2b-transgenic EAE model (Ji et al., 2013). The same inhibitor attenuates anti-glomerular basement membrane activity in a Goodpasture model (Huynh et al., 2019). In both studies, DR2a was not considered, and one may speculate that single small molecules blocking both alleles or combining blockers for DR2a and DR2b could be explored as immunotherapy for MS. Future studies should address whether our observations hold for other MS autoantigens, such as myelin peptides and the recently discovered non-myelin protein guanosine diphosphate (GDP) L-fucose synthase, which is recognized by brain-infiltrating T cells and has similarities to GDP L-fucose synthase homologs of certain gut microbiota, most notably *Akkermansia* (Planas et al., 2018).

STAR★METHODS

Detailed methods are provided in the online version of this paper and include the following:

- KEY RESOURCES TABLE
- RESOURCE AVAILABILITY
  - Lead Contact
  - Materials Availability
  - Data and Code Availability
- EXPERIMENTAL MODEL AND SUBJECT DETAILS
  - Human subjects
  - Cell lines
  - Primary cells
- METHOD DETAILS
  - DNA extraction and HLA genotyping
  - Isolation of TECs from thymic tissues
  - Generation of DR2a and DR2b allele-specific monoclonal antibodies
  - Immunofluorescence
  - Immunopeptidome isolation and analysis
  - Proliferation assay
  - Cytokine measurement
  - Flow cytometric analysis
  - T cell cloning and identification
  - Gene expression of TCC14 after peptide stimulation
  - RNA extraction and sequencing
  - Positional scanning synthetic combinatorial peptide libraries (ps-SCL) and biometrical analysis
- QUANTIFICATION AND STATISTICAL ANALYSIS

AUTHOR CONTRIBUTIONS

J.W. designed, performed, and analyzed experiments; performed statistical analyses; interpreted the data; and contributed to writing the manuscript. I.J. designed, performed, and analyzed experiments and interpreted the data. L.M., H.-G.R., and S.S. performed immunopeptidome isolation and preliminary data analyses. V.H. and M.H.-H. collected thymic tissues for immunopeptidome analysis, isolated thymic APCs for RNA sequencing, and interpreted thymic immunopeptidome data. R.R. and L.F.-F. provided brain tissue for immunopeptidome analyses. N.C.T. and Y.Z. created protein databases and provided the tool for peptide searching. L.O. performed analysis of RNA sequencing data. C.C. isolated and expanded the CSF-infiltrating CD4$^+$ T cells. M.F. prepared all ethics documents. W.F. provided technical support for the experiments. R.N. prepared the peptide pools of MS target proteins. T.M.C.B. and T.E. were involved in HLA typing and interpretation of HLA associations. W.W.K. generated BLS-DR2a and -DR2b cells. J.T.N. and J.-H.L. generated allele-specific monoclonal antibodies. C.M. assisted with choosing EBV peptides for cross-reactivity studies. M.S. provided expertise regarding epitope identification and interpretation of T cell data. R.M. designed the overall study and experiments and supervised them, interpreted the data, and wrote the manuscript. I.J., N.C.T., C.M., H.-G.R., M.S., and R.R. edited the manuscript.

DECLARATION OF INTERESTS

REFERENCES

Adair, P., Kim, Y.C., Pratt, K.P., and Scott, D.W. (2016). Avidity of human T cell receptor engineered CD4(+) T cells drives T-helper differentiation fate. Cell. Immunol. *299*, 30–41.

Adamopoulou, E., Tenzer, S., Hillen, N., Klug, P., Rota, I.A., Tietz, S., Gebhardt, M., Stevanovic, S., Schild, H., Tolosa, E., et al. (2013). Exploring the MHC-peptide matrix of central tolerance in the human thymus. Nat. Commun. *4*, 2039.

Albani, S., Keystone, E.C., Nelson, J.L., Ollier, W.E., La Cava, A., Montemayor, A.C., Weber, D.A., Montecucco, C., Martini, A., and Carson, D.A. (1995). Positive selection in autoimmunity: abnormal immune responses to a bacterial dnaJ antigenic determinant in patients with early rheumatoid arthritis. Nat. Med. *1*, 448–452.

Babicki, S., Arndt, D., Marcu, A., Liang, Y., Grant, J.R., Maciejewski, A., and Wishart, D.S. (2016). Heatmapper: web-enabled heat mapping for all. Nucleic Acids Res. *44* (W1), W147-53.

Balashov, K.E., Rottman, J.B., Weiner, H.L., and Hancock, W.W. (1999). CCR5(+) and CXCR3(+) T cells are increased in multiple sclerosis and their ligands MIP-1alpha and IP-10 are expressed in demyelinating brain lesions. Proc. Natl. Acad. Sci. USA *96*, 6873–6878.

Baum, H., Brusic, V., Choudhuri, K., Cunningham, P., Vergani, D., and Peakman, M. (1995a). MHC molecular mimicry in diabetes. Nat. Med. *1*, 388.

Baum, H., Wilson, C., Tiwana, H., Ahmadi, K., and Ebringer, A. (1995b). HLA association with autoimmune disease: restricted binding or T-cell selection? Lancet *346*, 1042–1043.

Berer, K., Gerdes, L.A., Cekanaviciute, E., Jia, X., Xiao, L., Xia, Z., Liu, C., Klotz, L., Stauffer, U., Baranzini, S.E., et al. (2017). Gut microbiota from multiple sclerosis patients enables spontaneous autoimmune encephalomyelitis in mice. Proc. Natl. Acad. Sci. USA *114*, 10719–10724.

Bielekova, B., Sung, M.H., Kadom, N., Simon, R., McFarland, H., and Martin, R. (2004). Expansion and functional relevance of high-avidity myelin-specific CD4+ T cells in multiple sclerosis. J. Immunol. *172*, 3893–3904.

Blackwell, J.M., Jamieson, S.E., and Burgner, D. (2009). HLA and infectious diseases. Clin. Microbiol. Rev. *22*, 370–385.

Bottazzo, G.F., Pujol-Borrell, R., Hanafusa, T., and Feldmann, M. (1983). Role of aberrant HLA-DR expression and antigen presentation in induction of endocrine autoimmunity. Lancet *2*, 1115–1119.

Boyman, O., Létourneau, S., Krieg, C., and Sprent, J. (2009). Homeostatic proliferation and survival of naïve and memory T cells. Eur. J. Immunol. *39*, 2088–2094.

Brochet, X., Lefranc, M.P., and Giudicelli, V. (2008). IMGT/V-QUEST: the highly customized and integrated system for IG and TR standardized V-J and V-D-J sequence analysis. Nucleic Acids Res. *36*, W503-8.

Bruno, R., Sabater, L., Sospedra, M., Ferrer-Francesch, X., Escudero, D., Martínez-Cáceres, E., and Pujol-Borrell, R. (2002). Multiple sclerosis candidate autoantigens except myelin oligodendrocyte glycoprotein are transcribed in human thymus. Eur. J. Immunol. *32*, 2737–2747.

Burroughs, A.K., Butler, P., Sternberg, M.J., and Baum, H. (1992). Molecular mimicry in liver disease. Nature *358*, 377–378.

Cai, G., and Hafler, D.A. (2007). Multispecific responses by T cells expanded by endogenous self-peptide/MHC complexes. Eur. J. Immunol. *37*, 602–612.

Caillier, S.J., Briggs, F., Cree, B.A., Baranzini, S.E., Fernandez-Viña, M., Ramsay, P.P., Khan, O., Royal, W., 3rd, Hauser, S.L., Barcellos, L.F., and Oksenberg, J.R. (2008). Uncoupling the roles of HLA-DRB1 and HLA-DRB5 genes in multiple sclerosis. J. Immunol. *181*, 5473–5480.

Cavalli, G., Hayashi, M., Jin, Y., Yorgov, D., Santorico, S.A., Holcomb, C., Rastrou, M., Erlich, H., Tengesdal, I.W., Dagna, L., et al. (2016). MHC class II super-enhancer increases surface expression of HLA-DR and HLA-DQ and affects cytokine production in autoimmune vitiligo. Proc. Natl. Acad. Sci. USA *113*, 1363–1368.

Cekanaviciute, E., Yoo, B.B., Runia, T.F., Debelius, J.W., Singh, S., Nelson, C.A., Kanner, R., Bencosme, Y., Lee, Y.K., Hauser, S.L., et al. (2017). Gut bacteria from multiple sclerosis patients modulate human T cells and exacerbate symptoms in mouse models. Proc. Natl. Acad. Sci. USA *114*, 10713–10718.

Chen, B.P., Madrigal, A., and Parham, P. (1990). Cytotoxic T cell recognition of an endogenous class I HLA peptide presented by a class II HLA molecule. J. Exp. Med. *172*, 779–788.

Chicz, R.M., Urban, R.G., Lane, W.S., Gorga, J.C., Stern, L.J., Vignali, D.A., and Strominger, J.L. (1992). Predominant naturally processed peptides bound to HLA-DR1 are derived from MHC-related molecules and are heterogeneous in size. Nature *358*, 764–768.

Chicz, R.M., Urban, R.G., Gorga, J.C., Vignali, D.A., Lane, W.S., and Strominger, J.L. (1993). Specificity and promiscuity among naturally processed peptides bound to HLA-DR alleles. J. Exp. Med. *178*, 27–47.

Colaert, N., Helsens, K., Martens, L., Vandekerckhove, J., and Gevaert, K. (2009). Improved visualization of protein consensus sequences by iceLogo. Nat. Methods 6, 786–787.

Cusick, M.F., Libbey, J.E., and Fujinami, R.S. (2012). Molecular mimicry as a mechanism of autoimmune disease. Clin. Rev. Allergy Immunol. 42, 102–111.

de Koster, H.S., Anderson, D.C., and Termijtelen, A. (1989). T cells sensitized to synthetic HLA-DR3 peptide give evidence of continuous presentation of denatured HLA-DR3 molecules by HLA-DP. J. Exp. Med. 169, 1191–1196.

Dendrou, C.A., Petersen, J., Rossjohn, J., and Fugger, L. (2018). HLA variation and disease. Nat. Rev. Immunol. 18, 325–339.

Dilthey, A.T., Moutsianas, L., Leslie, S., and McVean, G. (2011). HLA*IMP–an integrated framework for imputing classical HLA alleles from SNP genotypes. Bioinformatics 27, 968–972.

Enz, L.S., Zeis, T., Schmid, D., Geier, F., van der Meer, F., Steiner, G., Certa, U., Binder, T.M.C., Stadelmann, C., Martin, R., and Schaeren-Wiemers, N. (2019). Increased HLA-DR expression and cortical demyelination in MS links with HLA-DR15. Neurol. Neuroimmunol. Neuroinflamm. 7, e656.

Fogdell, A., Hillert, J., Sachs, C., and Olerup, O. (1995). The multiple sclerosis- and narcolepsy-associated HLA class II haplotype includes the DRB5*0101 allele. Tissue Antigens 46, 333–336.

Galperin, M., Farenc, C., Mukhopadhyay, M., Jayasinghe, D., Decroos, A., Benati, D., Tan, L.L., Ciacchi, L., Reid, H.H., Rossjohn, J., et al. (2018). CD4(+) T cell-mediated HLA class II cross-restriction in HIV controllers. Sci. Immunol. 3, eaat0687.

Gregersen, P.K., Silver, J., and Winchester, R.J. (1987). The shared epitope hypothesis. An approach to understanding the molecular genetics of susceptibility to rheumatoid arthritis. Arthritis Rheum. 30, 1205–1213.

Gregersen, J.W., Kranc, K.R., Ke, X., Svendsen, P., Madsen, L.S., Thomsen, A.R., Cardon, L.R., Bell, J.I., and Fugger, L. (2006). Functional epistasis on a common MHC haplotype associated with multiple sclerosis. Nature 443, 574–577.

Hauser, S.L., Waubant, E., Arnold, D.L., Vollmer, T., Antel, J., Fox, R.J., Bar-Or, A., Panzara, M., Sarkar, N., Agarwal, S., et al.; HERMES Trial Group (2008). B-cell depletion with rituximab in relapsing-remitting multiple sclerosis. N. Engl. J. Med. 358, 676–688.

Hemmer, B., Vergelli, M., Tranquill, L., Conlon, P., Ling, N., McFarland, H.F., and Martin, R. (1997). Human T-cell response to myelin basic protein peptide (83-99): extensive heterogeneity in antigen recognition, function, and phenotype. Neurology 49, 1116–1126.

Huynh, M., Eggenhuizen, P.J., Olson, G.L., Rao, N.B., Self, C.R., Sun, Y., Holdsworth, S.R., Kitching, A.R., and Ooi, J.D. (2019). HLA-DR15-specific inhibition attenuates autoreactivity to the Goodpasture antigen. J. Autoimmun. 103, 102276.

International Multiple Sclerosis Genetics Consortium (2018). Low-Frequency and Rare-Coding Variation Contributes to Multiple Sclerosis Risk. Cell 175, 1679–1687.e7.

International Multiple Sclerosis Genetics Consortium (2019). Multiple sclerosis genomic map implicates peripheral immune cells and microglia in susceptibility. Science 365, eaav7188.

Jangi, S., Gandhi, R., Cox, L.M., Li, N., von Glehn, F., Yan, R., Patel, B., Mazzola, M.A., Liu, S., Glanz, B.L., et al. (2016). Alterations of the human gut microbiome in multiple sclerosis. Nat. Commun. 7, 12015.

Jelcic, I., Al Nimer, F., Wang, J., Lentsch, V., Planas, R., Jelcic, I., Madjovski, A., Ruhrmann, S., Faigle, W., Frauenknecht, K., et al. (2018). Memory B Cells Activate Brain-Homing, Autoreactive CD4(+) T Cells in Multiple Sclerosis. Cell 175, 85–100. e23.

Jensen, K.K., Andreatta, M., Marcatili, P., Buus, S., Greenbaum, J.A., Yan, Z., Sette, A., Peters, B., and Nielsen, M. (2018). Improved methods for predicting peptide binding affinity to MHC class II molecules. Immunology 154, 394–406.

Jersild, C., Fog, T., Hansen, G.S., Thomsen, M., Svejgaard, A., and Dupont, B. (1973). Histocompatibility determinants in multiple sclerosis, with special reference to clinical course. Lancet 2, 1221–1225.

Ji, N., Somanaboeina, A., Dixit, A., Kawamura, K., Hayward, N.J., Self, C., Olson, G.L., and Forsthuber, T.G. (2013). Small molecule inhibitor of antigen binding and presentation by HLA-DR2b as a therapeutic strategy for the treatment of multiple sclerosis. J. Immunol. 191, 5074–5084.

Klein, L., Klugmann, M., Nave, K.A., Tuohy, V.K., and Kyewski, B. (2000). Shaping of the autoreactive T-cell repertoire by a splice variant of self protein expressed in thymic epithelial cells. Nat. Med. 6, 56–61.

Klein, L., Kyewski, B., Allen, P.M., and Hogquist, K.A. (2014). Positive and negative selection of the T cell repertoire: what thymocytes see (and don't see). Nat. Rev. Immunol. 14, 377–391.

Kourilsky, P., and Claverie, J.M. (1989). MHC restriction, alloreactivity, and thymic education: a common link? Cell 56, 327–329.

Krogsgaard, M., Li, Q.J., Sumen, C., Huppa, J.B., Huse, M., and Davis, M.M. (2005). Agonist/endogenous peptide-MHC heterodimers drive T cell activation and sensitivity. Nature 434, 238–243.

Kular, L., Liu, Y., Ruhrmann, S., Zheleznyakova, G., Marabita, F., Gomez-Cabrero, D., James, T., Ewing, E., Lindén, M., Górnikiewicz, B., et al. (2018). DNA methylation as a mediator of HLA-DRB1*15:01 and a protective variant in multiple sclerosis. Nat. Commun. 9, 2397.

Lang, H.L., Jacobsen, H., Ikemizu, S., Andersson, C., Harlos, K., Madsen, L., Hjorth, P., Sondergaard, L., Svejgaard, A., Wucherpfennig, K., et al. (2002). A functional and structural basis for TCR cross-reactivity in multiple sclerosis. Nat. Immunol. 3, 940–943.

Li, Y., Li, H., Martin, R., and Mariuzza, R.A. (2000). Structural basis for the binding of an immunodominant peptide from myelin basic protein in different registers by two HLA-DR2 proteins. J. Mol. Biol. 304, 177–188.

Li, Y., Huang, Y., Lue, J., Quandt, J.A., Martin, R., and Mariuzza, R.A. (2005). Structure of a human autoimmune TCR bound to a myelin basic protein self-peptide and a multiple sclerosis-associated MHC class II molecule. EMBO J. 24, 2968–2979.

Li, R., Rezk, A., Miyazaki, Y., Hilgenberg, E., Touil, H., Shen, P., Moore, C.S., Michel, L., Althekair, F., Rajasekharan, S., et al.; Canadian B cells in MS Team (2015). Proinflammatory GM-CSF-producing B cells in multiple sclerosis and B cell depletion therapy. Sci. Transl. Med. 7, 310ra166.

Lünemann, J.D., Kamradt, T., Martin, R., and Münz, C. (2007). Epstein-barr virus: environmental trigger of multiple sclerosis? J. Virol. 81, 6777–6784.

Marcu, A., Bichmann, L., Kuchenbecker, L., Backert, L., Kowalewski, D.J., Freudenmann, L.K., Löffler, M.W., Lübke, M., Walz, J.S., Velz, J., et al. (2019). The HLA Ligand Atlas. A resource of natural HLA ligands presented on benign tissues. bioRxiv. https://doi.org/10.1101/778944.

Martin, R., Howell, M.D., Jaraquemada, D., Flerlage, M., Richert, J., Brostoff, S., Long, E.O., McFarlin, D.E., and McFarland, H.F. (1991). A myelin basic protein peptide is recognized by cytotoxic T cells in the context of four HLA-DR types associated with multiple sclerosis. J. Exp. Med. 173, 19–24.

Mohme, M., Hotz, C., Stevanovic, S., Binder, T., Lee, J.H., Okoniewski, M., Eiermann, T., Sospedra, M., Rammensee, H.G., and Martin, R. (2013). HLA-DR15-derived self-peptides are involved in increased autologous T cell proliferation in multiple sclerosis. Brain 136, 1783–1798.

Molnarfi, N., Schulze-Topphoff, U., Weber, M.S., Patarroyo, J.C., Prod'homme, T., Varrin-Doyer, M., Shetty, A., Linington, C., Slavin, A.J., Hidalgo, J., et al. (2013). MHC class II-dependent B cell APC function is required for induction of CNS autoimmunity independent of myelin-specific antibodies. J. Exp. Med. 210, 2921–2937.

Moutsianas, L., Jostins, L., Beecham, A.H., Dilthey, A.T., Xifara, D.K., Ban, M., Shah, T.S., Patsopoulos, N.A., Alfredsson, L., Anderson, C.A., et al.; International IBD Genetics Consortium (IIBDGC) (2015). Class II HLA interactions modulate genetic risk for multiple sclerosis. Nat. Genet. 47, 1107–1113.

Muraro, P.A., Vergelli, M., Kalbus, M., Banks, D.E., Nagle, J.W., Tranquill, L.R., Nepom, G.T., Biddison, W.E., McFarland, H.F., and Martin, R. (1997). Immunodominance of a low-affinity major histocompatibility complex-binding myelin basic protein epitope (residues 111-129) in HLA-DR4 (B1*0401) subjects is associated with a restricted T cell receptor repertoire. J. Clin. Invest. 100, 339–349.

Nelde, A., Kowalewski, D.J., and Stevanović, S. (2019). Purification and Identification of Naturally Presented MHC Class I and II Ligands. Methods Mol. Biol. *1988*, 123–136.

Oksenberg, J.R., Baranzini, S.E., Sawcer, S., and Hauser, S.L. (2008). The genetics of multiple sclerosis: SNPs to pathways to pathogenesis. Nat. Rev. Genet. *9*, 516–526.

Oliveros, J.C. (2007–2015). Venny. An interactive tool for comparing lists with Venn's diagrams. https://bioinfogp.cnb.csic.es/tools/venny/index.html.

Olsson, T., Barcellos, L.F., and Alfredsson, L. (2017). Interactions between genetic, lifestyle and environmental risk factors for multiple sclerosis. Nat. Rev. Neurol. *13*, 25–36.

Ostrov, D.A., Alkanani, A., McDaniel, K.A., Case, S., Baschal, E.E., Pyle, L., Ellis, S., Pöllinger, B., Seidl, K.J., Shah, V.N., et al. (2018). Methyldopa blocks MHC class II binding to disease-specific antigens in autoimmune diabetes. J. Clin. Invest. *128*, 1888–1902.

Perez-Riverol, Y., Csordas, A., Bai, J., Bernal-Llinares, M., Hewapathirana, S., Kundu, D.J., Inuganti, A., Griss, J., Mayer, G., Eisenacher, M., et al. (2019). The PRIDE database and related tools and resources in 2019: improving support for quantification data. Nucleic Acids Res. *47* (D1), D442–D450.

Pette, M., Fujita, K., Wilkinson, D., Altmann, D.M., Trowsdale, J., Giegerich, G., Hinkkanen, A., Epplen, J.T., Kappos, L., and Wekerle, H. (1990). Myelin autoreactivity in multiple sclerosis: recognition of myelin basic protein in the context of HLA-DR2 products by T lymphocytes of multiple-sclerosis patients and healthy donors. Proc. Natl. Acad. Sci. USA *87*, 7968–7972.

Pinilla, C., Appel, J.R., and Houghten, R.A. (1994). Investigation of antigen-antibody interactions using a soluble, non-support-bound synthetic decapeptide library composed of four trillion (4 x 10(12) sequences. Biochem. J. *301*, 847–853.

Planas, R., Jelčić, I., Schippling, S., Martin, R., and Sospedra, M. (2012). Natalizumab treatment perturbs memory- and marginal zone-like B-cell homing in secondary lymphoid organs in multiple sclerosis. Eur. J. Immunol. *42*, 790–798.

Planas, R., Metz, I., Ortiz, Y., Vilarrasa, N., Jelčić, I., Salinas-Riester, G., Heesen, C., Brück, W., Martin, R., and Sospedra, M. (2015). Central role of Th2/Tc2 lymphocytes in pattern II multiple sclerosis lesions. Ann. Clin. Transl. Neurol. *2*, 875–893.

Planas, R., Santos, R., Tomas-Ojer, P., Cruciani, C., Lutterotti, A., Faigle, W., Schaeren-Wiemers, N., Espejo, C., Eixarch, H., Pinilla, C., et al. (2018). GDP-l-fucose synthase is a CD4⁺ T cell-specific autoantigen in DRB3*02:02 patients with multiple sclerosis. Sci. Transl. Med. *10*, eaat4301.

Prat, E., Tomaru, U., Sabater, L., Park, D.M., Granger, R., Kruse, N., Ohayon, J.M., Bettinotti, M.P., and Martin, R. (2005). HLA-DRB5*0101 and -DRB1*1501 expression in the multiple sclerosis-associated HLA-DR15 haplotype. J. Neuroimmunol. *167*, 108–119.

Quandt, J.A., Huh, J., Baig, M., Yao, K., Ito, N., Bryant, M., Kawamura, K., Pinilla, C., McFarland, H.F., Martin, R., and Ito, K. (2012). Myelin basic protein-specific TCR/HLA-DRB5*01:01 transgenic mice support the etiologic role of DRB5*01:01 in multiple sclerosis. J. Immunol. *189*, 2897–2908.

Reboldi, A., Coisne, C., Baumjohann, D., Benvenuto, F., Bottinelli, D., Lira, S., Uccelli, A., Lanzavecchia, A., Engelhardt, B., and Sallusto, F. (2009). C-C chemokine receptor 6-regulated entry of TH-17 cells into the CNS through the choroid plexus is required for the initiation of EAE. Nat. Immunol. *10*, 514–523.

Reich, D.S., Lucchinetti, C.F., and Calabresi, P.A. (2018). Multiple Sclerosis. N. Engl. J. Med. *378*, 169–180.

Robbins, F., Hurley, C.K., Tang, T., Yao, H., Lin, Y.S., Wade, J., Goeken, N., and Hartzman, R.J. (1997). Diversity associated with the second expressed HLA-DRB locus in the human population. Immunogenetics *46*, 104–110.

Rudensky, Y., Preston-Hurlburt, P., Hong, S.C., Barlow, A., and Janeway, C.A., Jr. (1991). Sequence analysis of peptides bound to MHC class II molecules. Nature *353*, 622–627.

Sabatino, J.J., Jr., Pröbstel, A.K., and Zamvil, S.S. (2019). B cells in autoimmune and neurodegenerative central nervous system diseases. Nat. Rev. Neurosci. *20*, 728–745.

Sawcer, S., Hellenthal, G., Pirinen, M., Spencer, C.C., Patsopoulos, N.A., Moutsianas, L., Dilthey, A., Su, Z., Freeman, C., Hunt, S.E., et al.; International Multiple Sclerosis Genetics Consortium; Wellcome Trust Case Control Consortium 2 (2011). Genetic risk and a primary role for cell-mediated immune mechanisms in multiple sclerosis. Nature *476*, 214–219.

Scally, S.W., Petersen, J., Law, S.C., Dudek, N.L., Nel, H.J., Loh, K.L., Wijeyewickrema, L.C., Eckle, S.B., van Heemst, J., Pike, R.N., et al. (2013). A molecular basis for the association of the HLA-DRB1 locus, citrullination, and rheumatoid arthritis. J. Exp. Med. *210*, 2569–2582.

Scholz, E.M., Marcilla, M., Daura, X., Arribas-Layton, D., James, E.A., and Alvarez, I. (2017). Human Leukocyte Antigen (HLA)-DRB1*15:01 and HLA-DRB5*01:01 Present Complementary Peptide Repertoires. Front. Immunol. *8*, 984.

Shahi, S.K., Freedman, S.N., Murra, A.C., Zarei, K., Sompallae, R., Gibson-Corley, K.N., Karandikar, N.J., Murray, J.A., and Mangalam, A.K. (2019). *Prevotella histicola*, A Human Gut Commensal, Is as Potent as COPAXONE® in an Animal Model of Multiple Sclerosis. Front. Immunol. *10*, 462.

Smith, K.J., Pyrdol, J., Gauthier, L., Wiley, D.C., and Wucherpfennig, K.W. (1998). Crystal structure of HLA-DR2 (DRA*0101, DRB1*1501) complexed with a peptide from human myelin basic protein. J. Exp. Med. *188*, 1511–1520.

Sospedra, M., and Martin, R. (2005). Immunology of multiple sclerosis. Annu. Rev. Immunol. *23*, 683–747.

Sospedra, M., Muraro, P.A., Stefanová, I., Zhao, Y., Chung, K., Li, Y., Giulianotti, M., Simon, R., Mariuzza, R., Pinilla, C., and Martin, R. (2006). Redundancy in antigen-presenting function of the HLA-DR and -DQ molecules in the multiple sclerosis-associated HLA-DR2 haplotype. J. Immunol. *176*, 1951–1961.

Sospedra, M., Zhao, Y., Giulianotti, M., Simon, R., Pinilla, C., and Martin, R. (2010). Combining positional scanning peptide libraries, HLA-DR transfectants and bioinformatics to dissect the epitope spectrum of HLA class II cross-restricted CD4+ T cell clones. J. Immunol. Methods *353*, 93–101.

Southwood, S., Sidney, J., Kondo, A., del Guercio, M.F., Appella, E., Hoffman, S., Kubo, R.T., Chesnut, R.W., Grey, H.M., and Sette, A. (1998). Several common HLA-DR types share largely overlapping peptide binding repertoires. J. Immunol. *160*, 3363–3373.

Stefanová, I., Dorfman, J.R., and Germain, R.N. (2002). Self-recognition promotes the foreign antigen sensitivity of naive T lymphocytes. Nature *420*, 429–434.

Sundqvist, E., Bergström, T., Daialhosein, H., Nyström, M., Sundström, P., Hillert, J., Alfredsson, L., Kockum, I., and Olsson, T. (2014). Cytomegalovirus seropositivity is negatively associated with multiple sclerosis. Mult. Scler. *20*, 165–173.

Takaba, H., and Takayanagi, H. (2017). The Mechanisms of T Cell Selection in the Thymus. Trends Immunol. *38*, 805–816.

Taylor, G.S., Long, H.M., Brooks, J.M., Rickinson, A.B., and Hislop, A.D. (2015). The immunology of Epstein-Barr virus-induced disease. Annu. Rev. Immunol. *33*, 787–821.

Tengvall, K., Huang, J., Hellström, C., Kammer, P., Biström, M., Ayoglu, B., Lima Bomfim, I., Stridh, P., Butt, J., Brenner, N., et al. (2019). Molecular mimicry between Anoctamin 2 and Epstein-Barr virus nuclear antigen 1 associates with multiple sclerosis risk. Proc. Natl. Acad. Sci. USA *116*, 16955–16960.

Thompson, A.J., Banwell, B.L., Barkhof, F., Carroll, W.M., Coetzee, T., Comi, G., Correale, J., Fazekas, F., Filippi, M., Freedman, M.S., et al. (2018). Diagnosis of multiple sclerosis: 2017 revisions of the McDonald criteria. Lancet Neurol. *17*, 162–173.

Tiercy, J.M., Jeannet, M., and Mach, B. (1991). Oligonucleotide typing analysis for the linkage disequilibrium between the polymorphic DRB1 and DRB5 loci in DR2 haplotypes. Tissue Antigens *37*, 161–164.

Vergelli, M., Hemmer, B., Utz, U., Vogt, A., Kalbus, M., Tranquill, L., Conlon, P., Ling, N., Steinman, L., McFarland, H.F., and Martin, R. (1996). Differential activation of human autoreactive T cell clones by altered peptide ligands derived from myelin basic protein peptide (87-99). Eur. J. Immunol. *26*, 2624–2634.

Vergelli, M., Hemmer, B., Kalbus, M., Vogt, A.B., Ling, N., Conlon, P., Coligan, J.E., McFarland, H., and Martin, R. (1997). Modifications of peptide ligands enhancing T cell responsiveness imply large numbers of stimulatory ligands for autoreactive T cells. J. Immunol. *158*, 3746–3752.

Villadangos, J.A., and Ploegh, H.L. (2000). Proteolysis in MHC class II antigen presentation: who's in charge? Immunity *12*, 233–239.

Vogt, A.B., Kropshofer, H., Kalbacher, H., Kalbus, M., Rammensee, H.G., Coligan, J.E., and Martin, R. (1994). Ligand motifs of HLA-DRB5*0101 and DRB1*1501 molecules delineated from self-peptides. J. Immunol. *153*, 1665–1673.

Wucherpfennig, K.W., and Strominger, J.L. (1995). Molecular mimicry in T cell-mediated autoimmunity: viral peptides activate human T cell clones specific for myelin basic protein. Cell *80*, 695–705.

Wucherpfennig, K.W., Sette, A., Southwood, S., Oseroff, C., Matsui, M., Strominger, J.L., and Hafler, D.A. (1994). Structural requirements for binding of an immunodominant myelin basic protein peptide to DR2 isotypes and for its recognition by human T cell clones. J. Exp. Med. *179*, 279–290.

Yousef, S., Planas, R., Chakroun, K., Hoffmeister-Ullerich, S., Binder, T.M., Eiermann, T.H., Martin, R., and Sospedra, M. (2012). TCR bias and HLA cross-restriction are strategies of human brain-infiltrating JC virus-specific CD4+ T cells during viral infection. J. Immunol. *189*, 3618–3630.

Zhao, Y., Gran, B., Pinilla, C., Markovic-Plese, S., Hemmer, B., Tzou, A., Whitney, L.W., Biddison, W.E., Martin, R., and Simon, R. (2001). Combinatorial peptide libraries and biometric score matrices permit the quantitative analysis of specific and degenerate interactions between clonotypic TCR and MHC peptide ligands. J. Immunol. *167*, 2130–2141.

STAR★METHODS

KEY RESOURCES TABLE

REAGENT or RESOURCE	SOURCE	IDENTIFIER
Antibodies		
Purified DR2a allele-specific monoclonal antibody	Purchased under an agreement from One Lambda (Thermo Fisher Scientific)	N/A
Purified DR2b allele-specific monoclonal antibody	Purchased under an agreement from One Lambda (Thermo Fisher Scientific)	N/A
Alexa Fluor 488-conjugated DR2a-specific antibody	Purchased under an agreement from One Lambda (Thermo Fisher Scientific)	N/A
Alexa Fluor 647-conjugated DR2b-specific antibody	Purchased under an agreement from One Lambda (Thermo Fisher Scientific)	N/A
Goat anti-Mouse IgG1 Cross-Adsorbed Secondary Antibody, Alexa Fluor 488	Invitrogen	Cat# A-21121; RRID:AB_2535764
Goat anti-Mouse IgG2b Cross-Adsorbed Secondary Antibody, Alexa Fluor 647	Invitrogen	Cat# A-21242; RRID:AB_2535811
FITC anti-human CD69 antibody (clone FN50)	BD PharMingen	Cat# 555530; RRID:AB_395915
APC anti-human CD25 antibody (clone BC96)	Biolegend	Cat# 302610; RRID:AB_314280
PE/Cy7 anti-human TCR α/β antibody (clone IP26)	Biolegend	Cat# 306720; RRID:AB_10639947
Pacific Blue anti-human CD4 antibody (clone OKT4)	Biolegend	Cat# 317429; RRID:AB_1595438
PerCP/Cy5.5 anti-human CD3 antibody (clone OKT3)	Biolegend	Cat# 317336; RRID:AB_2561628
PE/Cy7 anti-human CD14 Antibody (clone 63D3)	Biolegend	Cat# 367112; RRID:AB_2566714
Alexa Fluor® 700 anti-human CD19 Antibody (clone HIB19)	Biolegend	Cat# 302226; RRID:AB_493751
APC anti-human CD45RA (clone HI100)	Biolegend	Cat# 304112; RRID:AB_314416
Alexa Fluor® 700 anti-human CD45 Antibody (clone 2D1)	Biolegend	Cat# 368514; RRID:AB_2566374
PerCP/Cyanine5.5 anti-human CD326 (EpCAM) Antibody (clone 9C4)	Biolegend	Cat# 324214; RRID:AB_2098808
APC/Fire 750 anti-human HLA-DR Antibody (clone L243)	Biolegend	Cat# 307658; RRID:AB_2572101
Pacific Blue anti-human CD8 Antibody (Clone SK1)	Biolegend	Cat# 344718; RRID:AB_10551438
Alexa Fluor® 700 anti-human CD183 (CXCR3) Antibody (Clone G025H7)	Biolegend	Cat# 353742; RRID:AB_2616920
Brilliant Violet 785 anti-human CD196 (CCR6) Antibody (Clone G034E3)	Biolegend	Cat# 353422; RRID:AB_2563660
PE anti-human HLA-DR Antibody (Clone L243)	Biolegend	Cat# 307606; RRID:AB_314684
Purified anti-human HLA-DR Antibody (Clone L243)	Provided by HG. Rammensee, University of Tubingen, Germany	N/A
TCR Vβ1-PE, BL37.2, 1 mL, ASR	Beckman Coulter	Cat# IM2355; RRID:AB_131329
TCR Vβ2-PE, MPB,2D5, 1 mL, ASR	Beckman Coulter	Cat# IM2213; RRID:AB_131311
TCR Vβ3-FITC, CH92, 1 mL, ASR	Beckman Coulter	Cat# IM2372; RRID:AB_131046
TCR Vβ5.1-FITC, IMMU 157, 1 mL, ASR	Beckman Coulter	Cat# IM1552; RRID:AB_131023
TCR Vβ5.2-FITC, 36213, 1 mL, ASR	Beckman Coulter	Cat# IM1482; RRID:AB_130872
TCR Vβ7.1-PE, ZOE, 1 mL, ASR	Beckman Coulter	Cat# IM2287; RRID:AB_131323
TCR Vβ8-FITC, 56C5.2, 1 mL, ASR	Beckman Coulter	Cat# IM1233; RRID:AB_130922
TCR Vβ9-PE, FIN9, 1 mL, ASR	Beckman Coulter	Cat# IM2003; RRID:AB_131193
TCR Vβ11-FITC, C21, 1 mL, ASR	Beckman Coulter	Cat# IM1586; RRID:AB_131027

(*Continued on next page*)

CellPress
OPEN ACCESS

Continued

REAGENT or RESOURCE	SOURCE	IDENTIFIER
TCR Vβ12-PE, VER2.32.1, 1 mL, ASR	Beckman Coulter	Cat# IM2291; RRID:AB_131198
TCR Vβ13.1-PE, IMMU 222, 1 mL, ASR	Beckman Coulter	Cat# IM2292; RRID:AB_131326
TCR Vβ13.6-FITC, JU74.3, 1 mL, ASR	Beckman Coulter	Cat# IM1330; RRID:AB_131012
TCR Vβ14-PE, CAS1.1.3, 1 mL, ASR	Beckman Coulter	Cat# IM2047; RRID:AB_131304
TCR Vβ16-FITC, TAMAYA1.2, 1 mL, ASR	Beckman Coulter	Cat# IM1560; RRID:AB_130875
TCR Vβ17-FITC, E17.5F3.15.13, 1 mL, ASR	Beckman Coulter	Cat# IM1234; RRID:AB_131007
TCR Vβ18-PE, BA62.6, 1 mL, ASR	Beckman Coulter	Cat# IM2049; RRID:AB_131305
TCR Vβ20-PE, ELL1.4, 1 mL, ASR	Beckman Coulter	Cat# IM2295; RRID:AB_131328
TCR Vβ21.3-FITC, IG125, 1 mL, ASR	Beckman Coulter	Cat# IM1483; RRID:AB_131021
TCR Vβ22-FITC, IMMU 546, 1 mL, ASR	Beckman Coulter	Cat# IM1484; RRID:AB_131022
TCR Vβ23-PE, AF23, 1 mL, ASR	Beckman Coulter	Cat# IM2004; RRID:AB_131302
TCR Vβ5.3-PE, 3D11, 1 mL, ASR	Beckman Coulter	Cat# IM2002; RRID:AB_131230
Purified Mouse IgG2a, κ Isotype Ctrl Antibody	Biolegend	Cat# 401502; RRID:AB_2800437
Biological Samples		
Peripheral blood	This paper	N/A
Peripheral blood	This paper	N/A
Leukaphereses from MS patients	This paper	N/A
Buffy coats from HDs	This paper	N/A
Thymic tissues	This paper	N/A
MS brain tissues	This paper	N/A
Cerebrospinal fluid (CSF)	This paper; Planas et al., 2018	N/A
Chemicals, Peptides, and Recombinant Proteins		
Bovine serum albumin (BSA)	Roth	Cat# 3854.3
Carboxyfluorescein diacetate N-succinimidyl ester (CFSE)	Sigma-Aldrich	Cat# 21888
Dimethyl sulfoxide (DMSO)	Applichem	Cat# A3672
Ficoll	Eurobio	Cat# GAUFIC0065
EDTA solution pH 8.0 (0.5 M)	AppliChem	Cat# A3145,1000
L-glutamine	Thermo Fisher Scientific	Cat# 25030024
Penicillin-Streptomycin Solution, 100x	Corning	Cat# 30-002-CI
Gentamicin	Sigma-Aldrich	Cat# G1397
Human IL-2 containing supernatant (produced with T6 cell line)	Provided by F. Sallusto, IRB, Bellinzona, Switzerland	N/A
Positional scanning synthetic combinatorial peptide libraries (ps-SCL, N-acetylated and C-amide, TPI 2040)	Pinilla et al., 1994	N/A
LIVE/DEAD Fixable Aqua Dead Cell Stain Kit	Thermo Fisher Scientific	Cat# L34957
Methyl-^{3}H-thymidine	Hartmann Analytic	Cat# M1762
Peptides	Peptides&Elephants	This paper, see also Table S5 and S7
Remel PHA Purified	Thermo Fisher Scientific	Cat# R30852801
QIAzol lysis reagent	QIAGEN	Cat# 79306
CEF II peptide pool	Peptides&Elephants	N/A
Phytohemagglutinin-L (PHA-L)	Sigma-Aldrich	Cat# L2769
Liberase TM Research Grade	Roche	Cat# 5401119001
DNase I, recombinant	Roche	Cat# 04536282001
Percoll	GE healthcare	Cat# 17-0891-01
Triton X-100	Sigma-Aldrich	Cat# T8787
Proteinase K	Roche	Cat# 03115879001

(Continued on next page)

Continued

REAGENT or RESOURCE	SOURCE	IDENTIFIER
MEM Non-Essential Amino Acids Solution (100X)	GIBCO	Cat# 11140050
Sodium Pyruvate (100 mM)	GIBCO	Cat# 11360070
2-Mercaptoethanol (50 mM)	GIBCO	Cat# 31350010
Poly-L-lysine solution	Sigma-Aldrich	Cat# P8920
Immunoglobulin G from human serum	Sigma-Aldrich	Cat# 56834
CHAPS	PanReac AppliChem	Cat# A1099.0050
cOmplete Protease Inhibitor Cocktail	Roche	Cat# 11697498001
Trifluoroacetic acid (TFA)	Sigma-Aldrich	Cat# 299537
RPMI-1640 medium	Sigma-Aldrich	Cat# R0883
X-Vivo medium	Lonza	Cat# BE04-418F
Fetal calf serum (FCS)	Eurobio	Cat# CVFSVF0001
Human serum	Blood Bank Basel, Switzerland	N/A
IMDM medium	GE healthcare	Cat# SH30259.01
Polyethylene glycol solution	Sigma-Aldrich	Cat# P7181
HAT Media Supplement (50 ×) Hybri-Max	Sigma-Aldrich	Cat# H0262
Fetal Bovine Serum	Corning	Cat# 35-010-CV
RPMI 1640 Medium	Thermo Fisher Scientific	Cat# 11875101
Penicillin-Streptomycin Solution	Thermo Fisher Scientific	Cat# 15140130
Critical Commercial Assays		
CD19 MicroBeads, human	Miltenyi Biotec	Cat# 130-050-301, RRID:AB_2848166
CD14 MicroBeads, human	Miltenyi Biotec	Cat# 130-050-201, RRID:AB_2665482
CD45RA MicroBeads, human	Miltenyi Biotec	Cat# 130-045-901
CD4 T Cell Isolation Kit, human	Miltenyi Biotec	Cat# 130-096-533
Pan Monocyte Isolation Kit, human	Miltenyi Biotec	Cat# 130-096-537
CD4 MicroBeads, human	Miltenyi Biotec	Cat# 130-045-101
ELISA MAX Standard Set Human IFN-γ	Biolegend	Cat# 430101
LEGENDplex Human T Helper Cytokine Panels	Biolegend	Cat# 740001, RRID:AB_2784515
T Cell Activation/Expansion Kit, human	Miltenyi Biotec	Cat# 130-091-441
Image-iT Fixation/Permeabilization Kit	Invitrogen	Cat# R37602
SlowFade Diamond Antifade Mountant with DAPI	Invitrogen	Cat# S36968
RNeasy Mini Kit (50)	QIAGEN	Cat# 74104
PCR Master Mix (2X)	Thermo Scientific	Cat# K0171
RevertAid First Strand cDNA Synthesis Kit	Thermo Scientific	Cat# K1621
Deposited Data		
RNA sequencing data of B cells and monocytes	This paper	ENA: PRJEB34207
RNA sequencing data of thymic epithelial cells (TECs)	This paper	ENA: PRJEB34209
RNA sequencing data of peptide-stimulated TCC14 cells	This paper	ENA: PRJEB35576
Amino acid sequences of the eluted peptides	This paper	ProteomeXchange Consortium: PXD015249
Immunopeptidomic data from tumor tissues, unaffected surrounding tissue, and blood samples	HLA Ligand Atlas	https://hla-ligand-atlas.org/search
Experimental Models: Cell Lines		
BLS-DR2a cells	Generated by B. Kwok, Benaroya Research Institute, Seattle	N/A
BLS-DR2b cells	Generated by B. Kwok, Benaroya Research Institute, Seattle	N/A
TCC3A6	Vergelli et al., 1996	N/A

Continued

REAGENT or RESOURCE	SOURCE	IDENTIFIER
TCC5F6	Vergelli et al., 1997	N/A
TCC14	Jelcic et al., 2018	N/A
Oligonucleotides		
Primer: TRBC Reverse: gacagcggaagtggttgcgggggt	Microsynth	N/A
Primer: TRBV3-1 Forward: cctaaatctccagacaaagc	Microsynth	N/A
Primer: TRBV12-3/4 Forward: tctggtacagacagaccatg	Microsynth	N/A
Software and Algorithms		
FlowJo	Tree Star	https://www.flowjo.com/ ; RRID: SCR_008520
GraphPad Prism 8.0	Graphpad	https://www.graphpad.com/ ; RRID: SCR_002798
ImageJ	NIH	https://imagej.nih.gov/ij/ ; RRID:SCR_003070
NetMHCII 2.3 Server	Jensen et al., 2018	http://www.cbs.dtu.dk/services/NetMHCII-2.3/
Venny2.1	Oliveros, J.C. (2007-2015) Venny. An interactive tool for comparing lists with Venn's diagrams.	https://bioinfogp.cnb.csic.es/tools/venny/index.html ; RRID:SCR_016561
IMGT/V-QUEST	Brochet et al., 2008	http://www.imgt.org/IMGT_vquest/vquest ; RRID:SCR_010749
iceLogo	Colaert et al., 2009	https://iomics.ugent.be/icelogoserver/ ; RRID:SCR_012137
Heatmapper	Babicki et al., 2016	http://www.heatmapper.ca/ ; RRID:SCR_016974

RESOURCE AVAILABILITY

Lead Contact

Further information and requests for resources and reagents should be directed to and will be fulfilled by the Lead Contact, Roland Martin (roland.martin@usz.ch).

Materials Availability

Reasonable amounts of antibodies generated in this study are available from the Lead Contact with a completed Material Transfer Agreement.

Data and Code Availability

The RNA sequencing raw data have been deposited to the European Nucleotide Archive (ENA; https://www.ebi.ac.uk/ena/browser/home) with the accession codes PRJEB34207, PRJEB34209, and PRJEB35576. The mass spectrometry immunopeptidomic raw data have been deposited to the ProteomeXchange Consortium (http://www.proteomexchange.org/) with the dataset identifier PXD015249. Immunopeptidomic data from tumor tissues, unaffected surrounding tissue, and blood samples are listed in the HLA Ligand Atlas (https://hla-ligand-atlas.org/search).

EXPERIMENTAL MODEL AND SUBJECT DETAILS

Human subjects

In a first cohort, peripheral blood samples from MS patients from the University Hospital Zurich, Zurich, Switzerland (n = 136; age range 21-70 (median 41), F:M ratio: 1.5) and the University Medical Center Hamburg-Eppendorf, Hamburg, Germany (n = 881; age range 20-79 (median 45), F:M ratio: 2.2) were collected for HLA genotyping. In a second cohort, leukaphereses or buffy coats were collected from 8 HDs, 4 RRMS, and 10 RRMS_NAT for HLA immunopeptidome analyses (HDs, n = 3; RRMS, n = 3; RRMS_NAT, n = 3), proliferation assays (HDs, n = 8; RRMS, n = 4; RRMS_NAT, n = 10), and T cell cloning (RRMS_NAT, n = 3). The detailed information of these samples is shown in Tables S1. Leukaphereses from MS patients were collected at the Hematology Clinic,

University Hospital Zurich, Zurich, Switzerland. Buffy coats from HDs were acquired from the Blutspende Zurich, Zurich, Switzerland. Thymic tissues from HLA-DR15$^+$ immunologically healthy children undergoing cardiac surgery were collected at the University Children's Hospital Zurich, Zurich, Switzerland (n = 4) for HLA immunopeptidome analyses (n = 4) and TEC isolation (n = 3). Highly inflamed MS brain tissues were collected from the UK MS Society Tissue Bank, Imperial College London, London, UK for HLA immunopeptidome analyses (n = 4). The detailed information of thymic and MS brain tissues is shown in Tables S4. MS was diagnosed according to the recent McDonald criteria (Thompson et al., 2018). The study was approved by the Cantonal Ethical Committee of Zurich, Switzerland (EC-No. of the research project 2013-0001, approved on 5th June 2013 and EC-No. of the ERC 2014-0699, approved on 27th February 2015). HLA genotyping of MS patients from Hamburg was approved under protocol No. 2758, Ethik Kommission der Ärztekammer Hamburg.

Cell lines

BLS-DR2a and BLS-DR2b cells originated from a bare lymphocyte syndrome (BLS) patient-derived B cell line transfected with the genes encoding DRA*01:01P/DRB5*01:01 (BLS-DR2a cells) or DRA*01:01P/ DRB1*15:01 (BLS-DR2b cells). BLS cells were expanded in RPMI-1640 medium (Sigma-Aldrich, Missouri, USA) containing 10% heat-inactivated fetal calf serum (FCS, Eurobio, Courtaboeuf, France), 2mM L-glutamine (Thermo Fisher Scientific, Massachusetts, USA), 100 U/ml penicillin (Corning, New York, USA), 100 μg/ml streptomycin (Corning), and 50 μg/mL gentamicin (Sigma-Aldrich).

TCC3A6, TCC5F6, and TCC14 were obtained from HLA-DR15$^+$ MS patients. TCC3A6 is MBP$_{(83-99)}$-specific and restricted by DR2a (Vergelli et al., 1996). Its TCR recognizes MBP$_{(83-99)}$ with low avidity (Li et al., 2005), but is encephalitogenic in a humanized transgenic mouse model (Quandt et al., 2012). TCC5F6 also recognizes MBP$_{(83-99)}$ but is restricted by DR2b (Vergelli et al., 1997). Both TCC3A6 and TCC5F6 are Th1 cells (Hemmer et al., 1997). TCC14 is a Th2 TCC generated from autoproliferating cells and clonally expanded in brain lesions of a pattern II MS patient (1175SA) (Jelcic et al., 2018; Planas et al., 2015). It is restricted by DR2b and responds to RASGRP2 that is an autoantigen identified by an unbiased epitope search (Zhao et al., 2001) and expressed by pro-inflammatory B cells and in the brain (Jelcic et al., 2018). The TCCs were expanded with irradiated allogeneic PBMCs (45 Gy), 1 μg/mL PHA (Sigma-Aldrich), and 20 U/ml human IL-2 (hIL-2 containing supernatant produced by T6 cell line that was kindly provided by F. Sallusto, IRB, Bellinzona, Switzerland) in IMDM medium (GE healthcare, Illinois, USA) containing 5% human serum (Blood Bank Basel, Switzerland), 2mM L-glutamine (Thermo Fisher Scientific), 100 U/ml penicillin (Corning), 100 μg/ml streptomycin (Corning), and 50 μg/mL gentamicin (Sigma-Aldrich). The medium was changed by aspirating half of the old medium and adding the same amount of fresh medium containing hIL-2 every 3-4 days for two weeks.

Primary cells

PBMCs were freshly isolated from leukaphereses or buffy coats using Ficoll (Eurobio) density gradient centrifugation. Isolated PBMCs were cryopreserved in freezing medium containing 90% heat-inactivated FCS (Eurobio) and 10% dimethyl sulfoxide (DMSO; Applichem, Darmstadt, Germany) and stored in liquid nitrogen.

CD4$^+$ T cells in the CSF of HLA-DR15$^+$ RRMS patients were purified by positive selection using CD4 microbeads, human (Miltenyi, Bergisch Gladbach, Germany). Isolated bulk CD4$^+$ T cells were seeded at 1.5×10^3 cells/well in 96-well U-bottom plates (Greiner Bio-One, Kremsmunster, Austria) together with 1.5×10^5 irradiated allogeneic PBMC (45Gy), 1 μg/ml PHA (REMEL, Thermo Fisher Scientific), and hIL-2 in RPMI-1640 medium containing 5% human serum (Blood Bank Basel), 2 mM glutamine (Thermo Fisher Scientific), 1% (vol/vol) nonessential amino acids (GIBCO, Thermo Fisher Scientific), 1% (vol/vol) sodium pyruvate (GIBCO), 5μM β-Mercaptoethanol (GIBCO), 100 U/ml penicillin (Corning), and 100 μg/ml streptomycin (Corning). The medium was changed by aspirating half of the old medium and adding the same amount of fresh medium containing hIL-2 every 3-4 days for up to 25 days until cells were fully rested.

METHOD DETAILS

DNA extraction and HLA genotyping

DNA was extracted from whole blood of MS patients using a standard DNA isolation protocol using Triton lysis buffer (Triton X-100, Sigma-Aldrich) and proteinase K (Roche, Basel, Switzerland). The genotype of HLA class I (A and B) and HLA class II (DRB1, DRB3, DRB4, DRB5, DQA1 and DQB1) alleles was determined using high-resolution HLA sequence-based typing (Histogenetics, New York, USA).

Isolation of TECs from thymic tissues

Thymic tissues from HLA-DR15$^+$ immunologically healthy children undergoing cardiac surgery were cleaned from necrotic and connective tissue and then minced using watchmaker forceps. Minced tissues were digested in 12 mL PBS containing 0.4 mg/ml Liberase TM (Roche) and 20 μg/ml DNase I (Roche) in a 37°C water bath with pipetting up and down frequently until the tissue was completely dissolved. Cells were washed in AutoMACS running buffer (Miltenyi) and enriched for antigen-presenting cells using Percoll (GE healthcare) gradient centrifugation. Enriched antigen-presenting cells were stained for surface markers using fluorochrome-conjugated antibodies, including anti-human CD45 antibody, anti-human CD326 (EpCAM) antibody, and anti-human HLA-DR antibody (Biolegend; Key Resources Table). 1.0×10^5 of HLA-DR$^+$ TECs (CD45$^-$EpCAM$^+$HLA-DR$^{int-high}$) were sorted

from enriched antigen-presenting cells using a FACSAria III 4L (BD Biosciences) and resuspended in Qiazol (QIAGEN, Hilden, Germany) for RNA extraction.

Generation of DR2a and DR2b allele-specific monoclonal antibodies

BALB/c mice were immunized and boosted with recombinant HLA-DRB5*01:01 antigen to obtain DR2a allele-specific monoclonal antibody. CB6F1 mice were immunized and boosted with BLS-DR2b cells to obtain DR2b allele-specific monoclonal antibody. In particular, the aim was to obtain high-affinity IgG antibodies. The antibody-producing splenocytes were isolated and fused with Sp2/0 myeloma cells as fusion partner via polyethylene glycol (Sigma-Aldrich) to form hybridomas. The hybridomas were then cultured with 100 μM hypoxathine, 0.4 μM aminopterin, and 16 μM thymidine (HAT, Sigma-Aldrich) in RPMI-1640 medium (Thermo Fisher Scientific) containing 10% Fetal Bovine Serum (FBS) (Corning), 2mM L-glutamine (Thermo Fisher Scientific), 100 U/ml penicillin (Thermo Fisher Scientific), and 100 μg/ml streptomycin (Thermo Fisher Scientific). Later, supernatants from hybridomas were collected and screened by cytotoxicity test and single antigen beads (One Lambda, Thermo Fisher Scientific) for DR2a and DR2b. Clones were screened by LABScreen single antigen HLA-II panel (One Lambda, Thermo Fisher Scientific) and picked based on immunoglobulin class and antigen specificity. Desired antibody-producing hybridomas were finally expanded *in vitro* and injected into the mouse to acquire ascitic fluid enriched for the specific antibodies. Characterization of reactivity against a broad panel of DR alleles is shown in Figure S1B. Purified DR2a- and DR2b-specific antibodies were acquired and used for immunopeptidome isolation and immunofluorescence. Alexa Fluor 488-conjugated DR2a-specific antibody and Alexa Fluor 647-conjugated DR2b-specific antibody were acquired and used for flow cytometric analysis.

Immunofluorescence

BLS-DR2a or BLS-DR2b cells were plated onto poly-L-Lysine (Sigma-Aldrich) -coated slides. The fixation, permeabilization, and blocking of nonspecific binding sites of the cells were performed using the Image-iT® Fix-Perm Kit (Invitrogen, California, USA) according to the manufacturer's instructions. The cells were then incubated with 10 μg/ml primary anti-DR2a or anti-DR2b antibody overnight at 4°C. Following several wash steps with PBS + 0.5% BSA, the cells were incubated with 1 μg/ml Alexa Fluor 488-conjugated goat anti-mouse IgG1 secondary antibody (Invitrogen) to target anti-DR2a antibody or 10 μg/ml Alexa Fluor 647-conjugated goat anti-mouse IgG2b secondary antibody (Invitrogen) to target anti-DR2b antibody for 1 h at room temperature. Thereafter, cells were washed several times with PBS + 0.5% BSA and mounted with SlowFade Diamond Antifade Mountant with DAPI (Invitrogen) and coverslips. The images were captured using fluorescence microscopy (Zeiss, Oberkochen, Germany) and analyzed using ImageJ (NIH).

Immunopeptidome isolation and analysis

For immunopeptidome isolation of blood B cells and monocytes, cryopreserved PBMCs from HLA-DR15+ donors were thawed and washed twice with serum-free X-VIVO 15™ medium (Lonza, Basel, Switzerland). B cells and monocytes were then purified by positive selection using CD19 microbeads, human (Miltenyi) and CD14 microbeads, human (Miltenyi) according to the manufacturer's instructions. Purified B cells and monocytes were collected and stored in −80°C until use. For the thymic tissues and highly inflamed MS brain tissues, immunopeptidomes were isolated directly using the frozen tissues.

To isolate the immunopeptidome presented by DR2a and DR2b, as previously described (Nelde et al., 2019), frozen B cell and monocyte pellets, thymic tissues, and MS brain tissues were lysed with 10 mM CHAPS (PanReac AppliChem, Darmstadt, Germany) with protease inhibitors (Roche) in PBS. The lysate was then ultrasonicated, and the supernatant was collected after centrifugation and clarified using 5 μm sterile filters (Millex®-SV low protein binding PVDF Durapore® syringe filter unit, Merck Millipore). The peptide/HLA complexes were isolated from the supernatant using an immunoprecipitation approach with the allele-specific antibodies, and peptides were eluted from HLA molecules with 0.2% Trifluoroacetic acid (TFA, Sigma-Aldrich). The peptides were separated from HLA molecules by ultracentrifugation using 10 kDa Amicon centrifugal filter units (Merck Millipore). The amino acid sequences of the eluted peptides were identified by liquid chromatography-tandem mass spectrometry (LC-MS/MS, LTQ Orbitrap XL). The mass spectrometry immunopeptidomic raw data have been deposited to the ProteomeXchange Consortium via the PRIDE (Perez-Riverol et al., 2019) partner repository with the dataset identifier PXD015249.

For the immunopeptidome analysis, the core binding motif and binding affinity of peptides to DR2a or DR2b were predicted using NetMHCII 2.3 Server (Jensen et al., 2018). Graphical representation of the core binding motif was generated using iceLogo (Colaert et al., 2009). The analyzed results are shown in Tables S2 and S3. The overlap of DR2a- and DR2b-presented unique peptides and the overlap of the source protein of DR2a- and DR2b-presented peptides between B cells and monocytes were analyzed using VENNY[2.1] (Oliveros, 2007–2015; https://bioinfogp.cnb.csic.es/tools/venny/index.html).

Proliferation assay

All peptides used in this study for stimulation purposes were synthesized with N-terminal acetylation and C-terminal amide (Peptides & Elephants, Hennigsdorf, Germany). RASGRP2$_{(78-87)}$: LVRYWISAFP; MBP$_{(83-99)}$: ENPVVHFFKNIVTPRT; VP1$_{(74-88)}$: NRDMLPCYSVARIPL; EBNA1$_{(482-496)}$: AEGLRALLARSHVER; TT$_{(830-844)}$: QYIKANSKFIGITEL; and TT$_{(947-967)}$: FNNFTVSFWLRVPKVSASHLE. HLA-DR-SPs used for synthesis are shown in Table S5.

For peptide stimulation assay of PBMCs, CD45RA⁻ PBMCs were recovered after negative selection using CD45RA microbeads, human (Miltenyi) according to the manufacturer's instruction. CD45RA⁻ PBMCs were seeded at 2×10^5 cells/well in 200 μl X-VIVO 15™ medium (Lonza) in 96-well U-bottom plates (Greiner Bio-One), and HLA-DR-SPs were then added at a final concentration of 10 μM. 10-15 replicate wells were performed per condition, and anti-CD2/CD3/CD28 antibody-loaded MACSibead particles (Miltenyi) were used as a positive control. A pan-HLA-DR-specific antibody (L243) was added under some conditions to block the function of HLA-DR molecules at a final concentration of 10 μg/ml. Proliferation was measured at day 7 by ³H-thymidine (Hartmann Analytic, Braunschweig, Germany) incorporation assay. The proliferation strength is depicted as counts per minute (cpm) or stimulatory index (SI). The SI indicates the ratio of cpm in the presence of the peptide versus cpm in the no peptide control.

To dissect the cell subsets in the proliferative compartment of CD45RA⁻ PBMCs after stimulating with HLA-DR-SPs, CD45RA⁻ PBMCs were isolated and then labeled with carboxyfluorescein succinimidyl ester (CFSE, Sigma-Aldrich). CFSE-labeled CD45RA⁻ PBMCs were seeded at 2×10^5 cells/well in 200 μl X-VIVO 15™ medium (Lonza) in 96-well U-bottom plates (Greiner Bio-One) and stimulated with HLA-DR-SPs pool. After 7 days, CFSE-labeled CD45RA⁻ PBMCs were collected and pooled from replicate wells, stained for Live/Dead® Aqua (Invitrogen) and surface markers, and acquired with an LSR Fortessa flow cytometer (BD Biosciences). Resulting data were analyzed using FlowJo (Tree Star).

To assess proliferation of blood CD4⁺ T cells upon co-culture with autologous monocytes, BLS-DR2a cells, or BLS-DR2b cells as APCs in the presence of HLA-DR-SPs, blood CD4⁺ T cells and monocytes were purified by negative selection using CD4⁺ T cell isolation kit, human (Miltenyi) and monocyte isolation kit, human (Miltenyi) according to the manufacturer's instruction. Purified blood CD4⁺ T cells were labeled prior to co-culture with CFSE (Sigma-Aldrich). CFSE-labeled blood CD4⁺ T cells (5×10^4 cells/well) were incubated with autologous monocytes, irradiated BLS-DR2a cells, or irradiated BLS-DR2b cells (1×10^5 cells/well) as APCs in 200 μl X-VIVO 15™ medium (Lonza) in 96-well U-bottom plates (Greiner Bio-One) and stimulated with HLA-DR-SPs pool at a final concentration of 10 μM. Anti-HLA-DR antibody (L243) was added under some conditions to block the interaction with HLA-DR molecules at a final concentration of 10 μg/ml. After 7 days, cells were collected and pooled from replicate wells and stained for Live/Dead® Aqua (Invitrogen) and surface markers. The proliferation of naive (CD45RA⁺) and memory (CD45RA⁻) CD4⁺ T cells was measured using an LSR Fortessa flow cytometer (BD Biosciences), and resulting data were analyzed using FlowJo (Tree Star).

For determining reactivity of CSF-infiltrating CD4⁺ T cells of HLA-DR15⁺ MS patients as shown in Table S6 to HLA-DR-SPs, CFSE-labeled CSF-infiltrating CD4⁺ T cells (5×10^4 cells/well) were incubated with irradiated BLS-DR2a cells or irradiated BLS-DR2b cells (1×10^5 cells/well) in 200 μl X-VIVO 15™ medium (Lonza) in 96-well U-bottom plates (Greiner Bio-One) and stimulated with HLA-DR-SPs pool at a final concentration of 10 μM. Anti-HLA-DR antibody (L243) was added under some conditions to block the interaction with HLA-DR molecules at a final concentration of 10 μg/ml. After 7 days, cells were collected and pooled from replicate wells and stained for Live/Dead® Aqua (Invitrogen) and surface markers. The proliferation of naive (CD45RA⁺) and memory (CD45RA⁻) CD4⁺ T cells was measured using an LSR Fortessa flow cytometer (BD Biosciences), and resulting data were analyzed using FlowJo (Tree Star).

For proliferation assays of autoreactive TCCs stimulating with HLA-DR-SPs, TCCs (2×10^4 cells/well) were seeded with irradiated BLS-DR2a or BLS-DR2b cells (5×10^4 cells/well) as APCs in 200 μl X-VIVO 15™ medium (Lonza) in 96-well U-bottom plates (Greiner Bio-One) and stimulated with HLA-DR-SPs pool at a final concentration of 10 μM. Cognate antigens were used as a positive control of stimulation. Proliferation was measured at day 3 by ³H-thymidine (Hartmann Analytic) incorporation assay.

Cytokine measurement

Supernatants were harvested from CD45RA⁻ PBMCs, bulk CD4⁺ T cells, CSF-infiltrating CD4⁺ T cells at day 7 or from TCCs at day 3 after peptide stimulation. Cytokines in the supernatants were measured with a bead-based immunoassay using LEGENDplex Multi-analyte Flow Assay kit (Biolegend, California, USA; Human Th cytokine panel (13-plex) includes IFN-γ, TNF-α, IL-2, -4, -5, -6, -9, -10, -13, -17A, -17F, -21, and -22) or with a ELISA using ELISA MAX Standard Set Human IFN-γ (Biolegend) according to the manufacturer's instructions.

Flow cytometric analysis

For analyzing DR2a and DR2b expression levels on B cells and monocytes, PBMCs from HLA-DR15⁺ donors were incubated with human IgG (Sigma-Aldrich) to block unspecific antibody binding to Fc-receptors, labeled with Live/Dead® Aqua (Invitrogen), and then stained for surface marker using fluorochrome-conjugated antibodies, including Alexa Fluor 488-conjugated anti-DR2a antibody (5 μg/ml, One Lambda, Thermo Fisher Scientific) and Alexa Fluor 647-conjugated anti-DR2b antibody (5 μg/ml, One Lambda, Thermo Fisher Scientific), at 4°C. For analyzing CD69, CD25, and TCR α/β expression on TCCs after stimulation, TCCs were harvested at different time points after stimulating with peptides and washed twice with PBS. TCCs were then incubated with human IgG (Sigma-Aldrich), labeled with Live/Dead® Aqua (Invitrogen), and stained for surface marker using fluorochrome-conjugated antibodies, including anti-human CD69 antibody, anti-human CD25 antibody, anti-human TCR α/β antibody, anti-human CD4 antibody, and anti-human CD3 antibody (Biolegend; Key Resources Table), at 4°C. Cells were washed twice after staining and resuspended with cold PBS containing 2mM ethylenediamine tetraacetic acid (EDTA, AppliChem) and 2% FCS (Eurobio). Measurement was performed using LSR Fortessa Flow Cytometer (BD Biosciences) and data were analyzed using FlowJo (Tree Star).

T cell cloning and identification

To generate $CD4^+$ TCCs that recognize both $RASGRP2_{(78-87)}$ and HLA-DR-SPs, PBMCs from 3 HLA-DR15$^+$ RRMS_NAT patients were stained with CFSE, and CD45RA$^-$ PBMCs were then isolated using CD45RA microbeads, human (Miltenyi) and stimulated with $RASGRP2_{(78-87)}$ at a concentration of 10μM. Proliferating (CFSE^{dim}) $CD4^+$ T cells were sorted at day 12 as single cells in 96-well U-bottom plates using SH800S Cell Sorter (Sony) and expanded with irradiated allogeneic PBMC (45 Gy), 1 μg/ml PHA (Sigma-Aldrich), and 20 U/ml hIL-2 in RPMI-1640 medium containing 5% heat-decomplemented human serum (Blood Bank Basel, Switzerland), 2mM L-glutamine (Thermo Fisher Scientific), 100 U/ml penicillin (Corning), 100 μg/ml streptomycin (Corning), and 50 μg/mL gentamicin (Sigma-Aldrich). The medium was changed by aspirating half of the old medium and adding the same amount of fresh medium containing hIL-2 every 3-4 days.

Expanded TCCs were co-cultured with irradiated autologous PBMCs as APCs and stimulated with $RASGRP2_{(78-87)}$ or HLA-DR-SPs to test their reactivity. TCCs that responded to both $RASGRP2_{(78-87)}$ and HLA-DR-SPs were chosen for further study. The phenotype of TCRVβ chain of TCCs was first assessed by flow cytometry using fluorochrome-conjugated antibodies (Beckman Coulter, USA; Key Resources Table) and further confirmed by sequencing. The sequencing results were analyzed using IMGT/V-QUEST (Brochet et al., 2008). The functional phenotype was analyzed by stimulating TCCs with anti-CD2/CD3/CD28 antibody-loaded MACSibead particles (Miltenyi) in X-VIVO 15^{TM} medium (Lonza), and after 3 days cytokines in supernatants were measured using LEGENDplex Multi-Analyte Flow Assay kit (Biolegend). The restriction of the TCCs was tested with irradiated BLS-DR2a or BLS-DR2b cells upon stimulation with $RASGRP2_{(78-87)}$, and proliferation of TCCs was measured at day 3 using ^{3}H-thymidine (Hartmann Analytic) incorporation assay.

Gene expression of TCC14 after peptide stimulation

TCC14 cells were co-cultured with BLS-DR2a or BLS-DR2b cells as APCs and stimulated with HLA-DR-SPs, peptides from EBV and *Akkermansia*, or $RASGRP2_{(78-87)}$ for 24 h. For each peptide, stimulation was performed with 10 replicate wells, and cells were pooled together after stimulation. After that, TCC14 cells were purified by negative selection using CD19 microbeads, human (Miltenyi) for RNA extraction and sequencing.

RNA extraction and sequencing

Blood B cells and monocytes from HDs and MS patients were purified by magnetic cell separation, TECs in thymic tissues from HLA-DR15$^+$ immunologically healthy children were isolated by sorter, and peptide-stimulated TCC14 cells were purified by magnetic cell separation as described above. Isolated cells were washed twice with PBS, and RNA extraction was performed using RNeasy Mini Kit (QIAGEN, Hilden, Germany) according to the manufacturer's instructions. RNA sequencing was performed using HiSeq 4000 or NovaSeq 6000 System (Illumina, California, USA) at the Functional Genomics Center Zurich (FGCZ). The RNA sequencing raw data have been deposited to the European Nucleotide Archive (ENA) with the accession codes PRJEB34207, PRJEB34209, and PRJEB35576. Heatmaps of the mRNA expression level of the essential proteases in antigen processing were generated using Heatmapper (Babicki et al., 2016). Heatmaps of the mRNA expression level in TCC14 cells were generated using R package ez-Run (FGCZ).

Positional scanning synthetic combinatorial peptide libraries (ps-SCL) and biometrical analysis

A L-amino acid decapeptide ps-SCL (N-acetylated and C-amide, TPI 2040) was prepared as described (Pinilla et al., 1994), which include 200 peptide mixtures as shown in Figure S6A. To test the reactivity with the library, TCC14 was co-cultured with irradiated BLS-DR2b cells as APCs and stimulated with each of the 200 peptide mixtures at a concentration of 200 μg/ml. The proliferation of TCC14 was measured after 72 h using ^{3}H-thymidine incorporation assay, and a scoring matrix was then generated based on the stimulatory potency of each peptide mixture. Using a biometrical analysis procedure generated before (Zhao et al., 2001), the scoring matrix was used to score all decapeptides of proteins encoded by EBV, HCMV, *Akkermansia*, and *Prevotella* from the National Center for Biotechnology Information (NCBI) Reference Sequence (RefSeq) database. The distribution of the scores of the decapeptides from EBV, HCMV, *Akkermansia*, and *Prevotella* were limited to a range of 20 to 125, with 190.88 being the highest possible score and 14.57 the lowest. ~30 peptides each from EBV, HCMV, *Akkermansia*, and *Prevotella* with high scores between 75 to 125 as shown in Table S7 were chosen to be synthesized (Peptides & Elephants), and the proliferative responses of TCC14 to these peptides determined using ^{3}H-thymidine (Hartmann Analytic) incorporation assay.

QUANTIFICATION AND STATISTICAL ANALYSIS

Statistical analyses were performed with GraphPad Prism 8.0. Unpaired t test and paired t test were used for statistical analyses between two groups. Correlation was calculated using Spearman's rank correlation test. The statistical tests used are reported in the figure legends. The value of n reported within figure legends represents number of donors. Data are expressed as mean or mean ± SEM, which are indicated in the figure legends. The data were considered statistically significant when differences achieved values of $p < 0.05$. The p values are reported in the figures where significant.
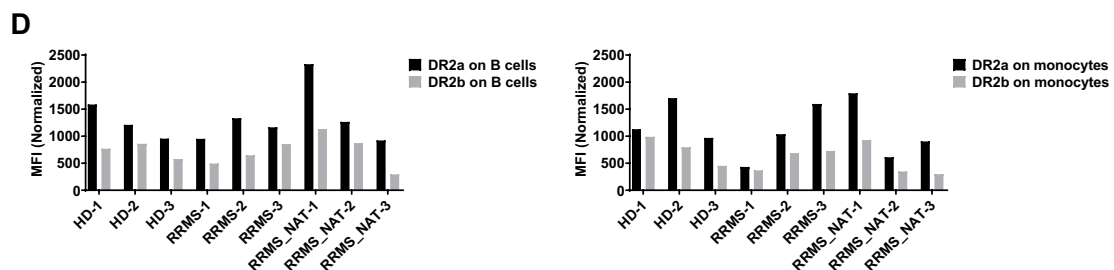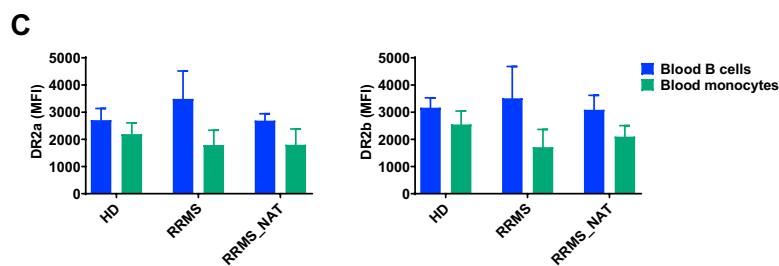
Supplemental Figures

A

Recombinant DRB5*01:01 antigen → Immunize mice → B cells + Myeloma cells → Hybridoma cell → Anti-DR2a antibody, IgG isotype → MFI: Cross-reactivity and affinity (DRB5*01:01 (DR2a), DRB1*15:01 (DR2b))

BLS-DR2b cells → Immunize mice → B cells + Myeloma cells → Hybridoma cell → Anti-DR2b antibody

B Allele reactivity of anti-DR2a antibody

Allele reactivity of anti-DR2b antibody

C DR2a (MFI) / DR2b (MFI) — HD, RRMS, RRMS_NAT; Blood B cells, Blood monocytes

D MFI (Normalized) — DR2a on B cells, DR2b on B cells; DR2a on monocytes, DR2b on monocytes
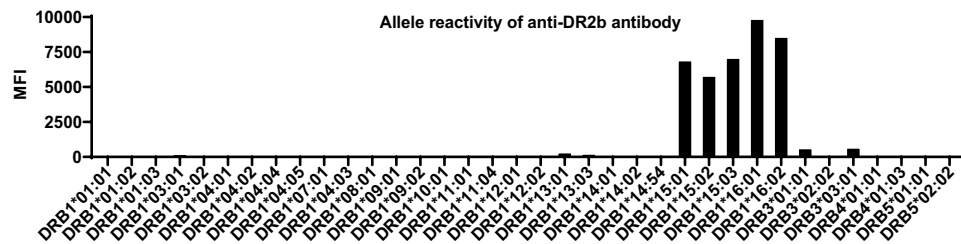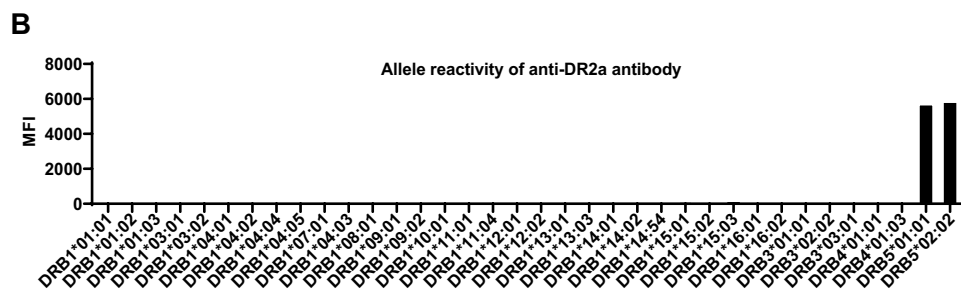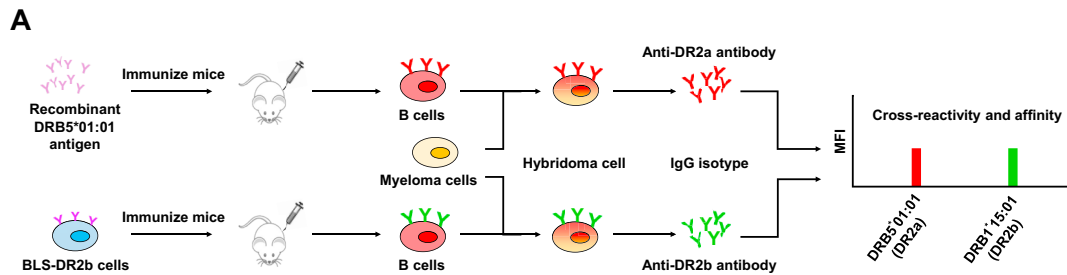
Figure S1. The Expression Level of DR2a Is Higher Than that of DR2b on Blood B Cells and Monocytes, Related to Figure 1 and Table S1

(A) Workflow diagram for the generation of DR2a (mIgG1 isotype) and DR2b (mIgG2b isotype) allele-specific monoclonal antibodies.

(B) Specificity of the DR2a and DR2b allele-specific monoclonal antibodies was examined with LABScreen™ system that uses microbeads coated with purified Class II HLA antigens and pre-optimized reagents for the detection of Class II HLA antibodies using flow cytometric technology.

(C) Expression levels of DR2a and DR2b on blood B cells and monocytes of HLA-DR15^{+} HDs (n = 3) and MS patients (RRMS, n = 3; RRMS_NAT, n = 3) were detected by flow cytometry using Alexa Fluor 488-conjugated DR2a-specific antibody and Alexa Fluor 647-conjugated DR2b-specific antibody.

(D) Normalized expression levels of DR2a and DR2b on blood B cells (left) and monocytes (right) from HLA-DR15^{+} HDs and MS patients were analyzed by flow cytometry using Alexa Fluor 488-conjugated DR2a-specific antibody and Alexa Fluor 647-conjugated DR2b-specific antibody. The PE-conjugated monomorphic antibody L243, which binds to the HLA-DR alpha chain and thus recognizes both DR2a and DR2b, was used to normalize the signals obtained with the two allele-specific antibodies. In brief, for the normalization, the ratios of the mean fluorescence intensity (MFI) of the allele-specific antibody versus the MFI of L243 on BLS-DR2a or BLS-DR2b cells were determined for each measurement. The resulting ratio was used to correct the MFI value of DR2a and DR2b expression on primary B cells and monocytes.
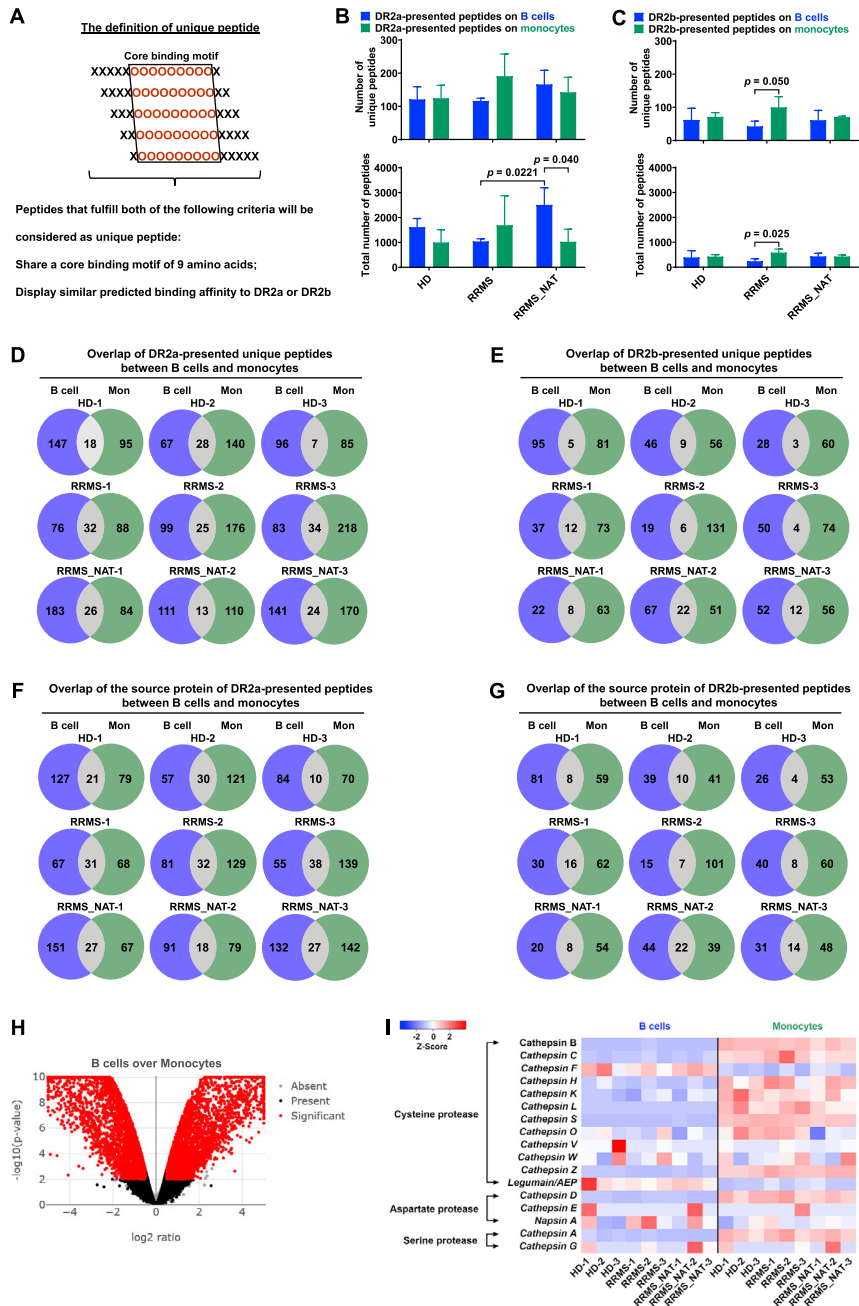
Data are expressed as mean ± SEM.

Figure S2. Low-Degree Overlaps of DR2a- or DR2b-Presented Unique Peptides and Their Source Proteins between B Cells and Monocytes, Related to Figure 1 and Tables S2 and S3

(A) Graphical illustration of the definition of unique peptides within this study.

(B) Comparison of the number of unique peptides (upper panel) and the total number of peptides (lower panel) eluted from DR2a between B cells and monocytes at the group level (HDs, n = 3; RRMS, n = 3; RRMS_NAT, n = 3).

(C) Comparison of the number of unique peptides (upper panel) and the total number of peptides (lower panel) eluted from DR2b between B cells and monocytes at the group level (HDs, n = 3; RRMS, n = 3; RRMS_NAT, n = 3).

(D-E) Overlap of the unique peptides presented by DR2a (D) or DR2b (E) between B cells and monocytes was analyzed at the individual's level (HDs, n = 3; RRMS, n = 3; RRMS_NAT, n = 3).

(F-G) Overlap of the source proteins of peptides presented by DR2a (F) or DR2b (G) between B cells and monocytes was analyzed at the individual's level (HDs, n = 3; RRMS, n = 3; RRMS_NAT, n = 3).

(H) Volcano plot of RNA sequencing results showing significantly differentially expressed genes between B cells and monocytes (log2 ratio > = 0.5 with p value ≤ 0.01). Present indicates genes with read counts > = 10 in more than one sample, absent indicates all genes that are not flagged as present, and significants indicates genes with |log2 ratio| > = 0.5 and p value ≤ 0.01.

(legend continued on next page)

(I) Heatmap showing the different expression levels of the genes of essential proteases in antigen processing in blood B cells and monocytes from HLA-DR15$^+$ HDs and MS patients.

Data are expressed as mean ± SEM, and p values were determined by unpaired t test.
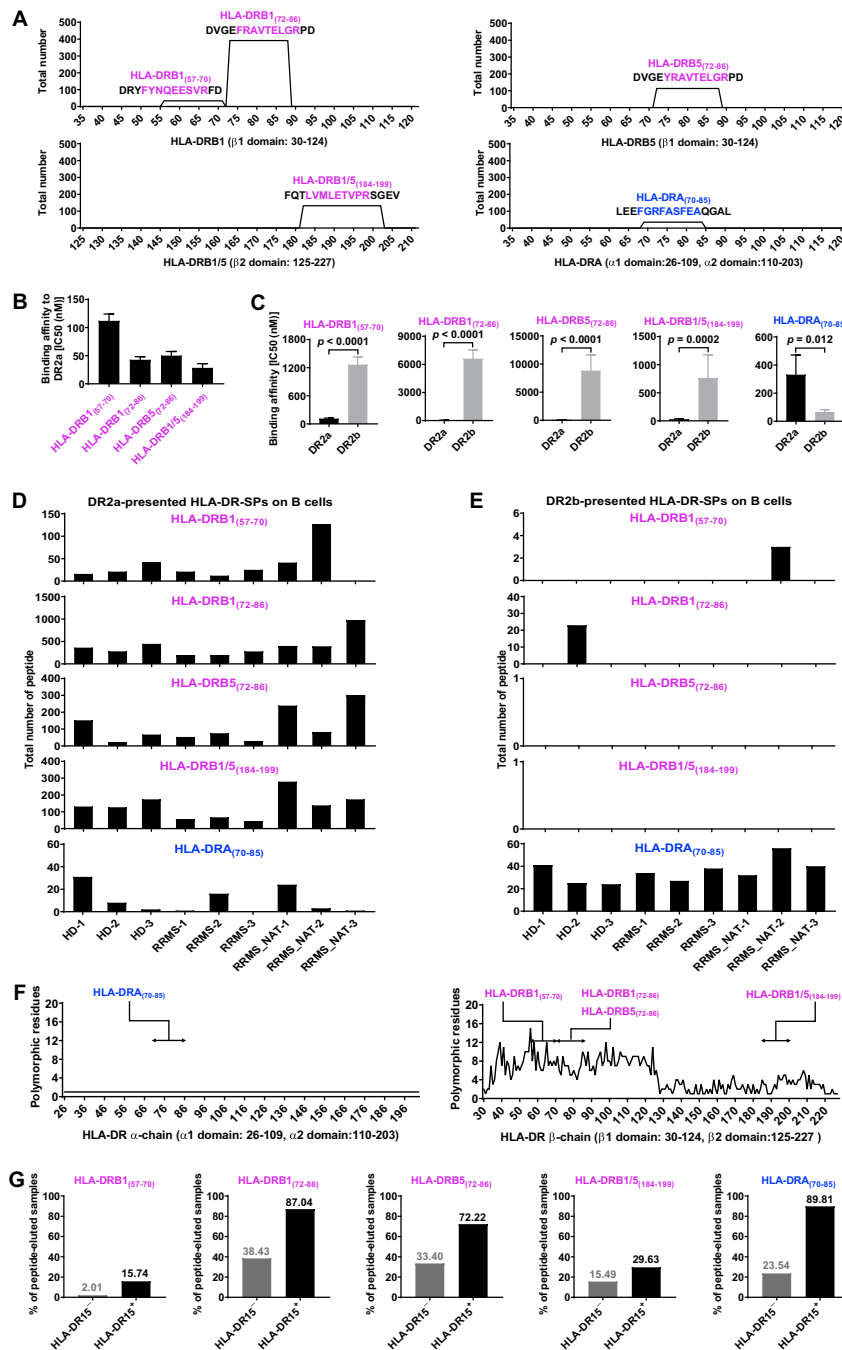
Figure S3. Sequence and Location of the Five Most Common HLA-DR-SPs Presented by DR2a and DR2b on Peripheral Blood B Cells, Related to Figure 2

(A) Total number and location within the HLA-DR α/β-chain sequences of the HLA-DR-SPs presented by DR2a or DR2b on B cells. Colored amino acids within peptide sequences represent the core binding motif, analyzed by NetMHCII 2.3 server. The total number of each peptide is expressed as mean.

(B) Comparison of the binding affinities, analyzed by NetMHCII 2.3 server, of the HLA-DR-β-SPs to DR2a.

(C) Comparison of the binding affinities of the HLA-DR-SPs to DR2a and DR2b.

(D) Total number of the five most common HLA-DR-SPs presented by DR2a on B cells.

(E) Total number of the five most common HLA-DR-SPs presented by DR2b on B cells.

(F) Variability of α- and β-chains of HLA-DR molecules. The y axis shows the number of polymorphic residues identified at each position of the α- or β-chains. Sequences were obtained from the European Bioinformatics Institute (EMBL-EBI). Origins of HLA-DR-α-SPs and HLA-DR-β-SPs are highlighted.

(G) Analyses of the immunopeptidomes presented by HLA-II molecules from a broad range of tumor tissues, unaffected tissues around the tumor, and blood samples. The anti-HLA-DR antibody (L243) and the anti-HLA-DR/DP/DQ antibody (Tü39) were used together to analyze the immunopeptidomes. The proportion of samples that include the five most common unique HLA-DR-SPs in HLA-DR15$^-$ samples (n = 497) and HLA-DR15$^+$ samples (n = 108) was calculated. Data are expressed as mean ± SEM, and p values were determined by unpaired t test.
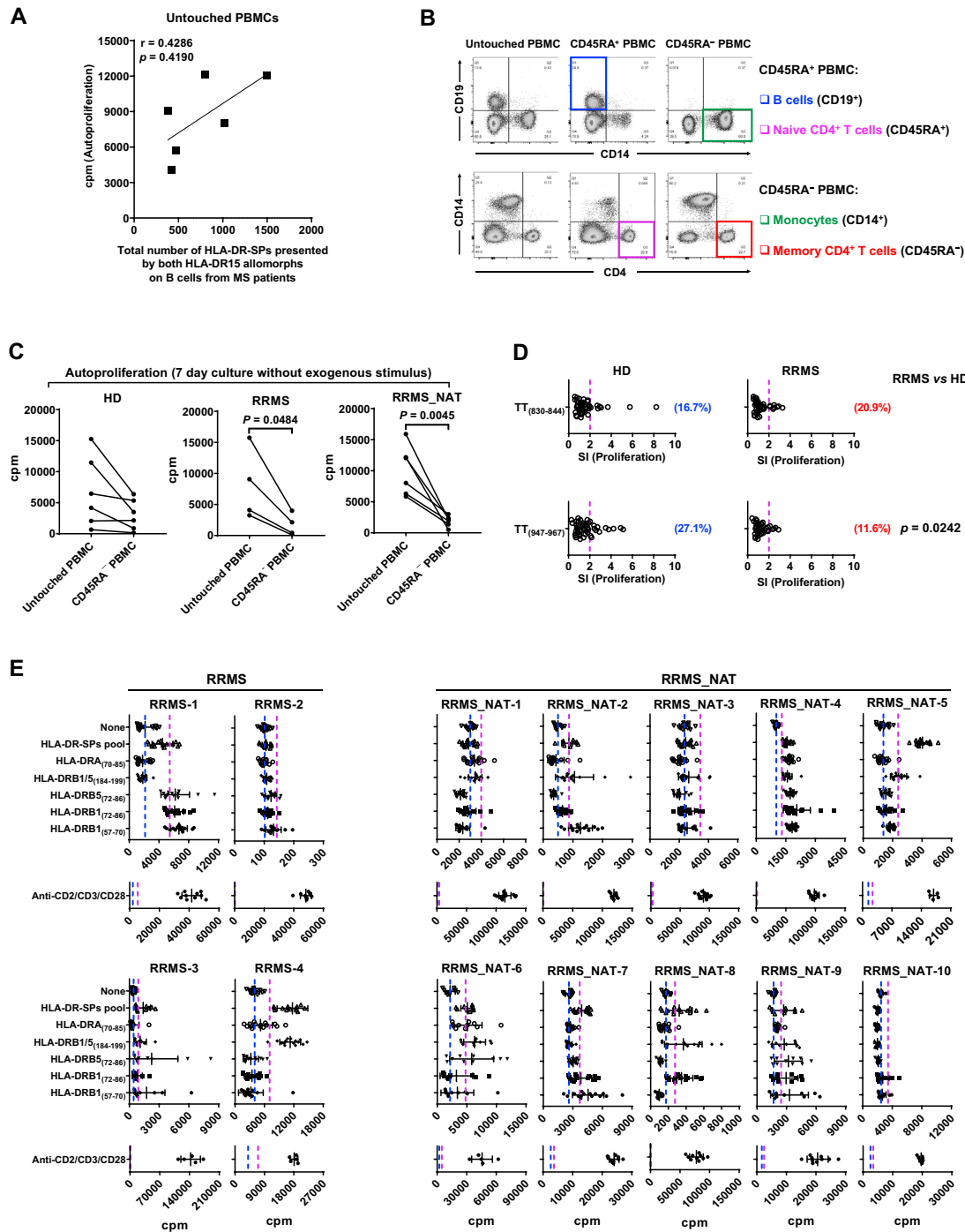
Figure S4. HLA-DR-SPs Mainly Activate Memory CD4+ T Cells in HLA-DR15+ MS Patients, Related to Figures 3 and 5 and Table S1

(A) Correlation of the total number of HLA-DR-SPs presented by the two HLA-DR15 molecules on B cells and the degree of autoproliferation in MS patients (RRMS, n = 3; RRMS_NAT, n = 3; Spearman's rank correlation test).

(B) PBMCs were separated into CD45RA+ cells and CD45RA− cells by magnetic cell isolation using CD45RA microbeads. Cell subsets in untouched PBMCs, CD45RA+ PBMCs, and CD45RA− PBMCs were analyzed by flow cytometry.

(C) Comparison of the autoproliferation between untouched PBMCs and CD45RA− PBMCs from HLA-DR15+ HDs (n = 6), RRMS (n = 4), or RRMS_NAT (n = 6). Data are expressed as mean, and p values were determined by paired t test.

(D) CD45RA− PBMCs from HLA-DR15+ HDs (n = 5) and MS patients (n = 5) were stimulated with Tetanus Toxin peptides, TT$_{(830-844)}$ and TT$_{(947-967)}$, which could be presented by DR2a and/or DR2b as previously reported. For each sample, each stimulation was performed with 10 replicate wells. Proliferations of CD45RA−

PBMCs were detected after 7 days by ^{3}H-thymidine incorporation assay, and the proliferation strength is depicted as SI. The p values were determined by unpaired t test.

(E) CD45RA$^-$ PBMCs from HLA-DR15$^+$ RRMS (n = 4) and RRMS_NAT (n = 10) patients were stimulated with the most common HLA-DR-SPs either alone or as pool. Proliferations of CD45RA$^-$ PBMCs were detected by ^{3}H-thymidine incorporation assay after 7 days, and proliferation strength is depicted as counts per minute (cpm). 10-15 replicate wells per condition are indicated by individual dots. The blue dotted line indicates the mean value of the no peptide control. The purple dotted line indicates the mean value plus three standard deviations of the no peptide control. Values above the purple dotted line were considered positive.
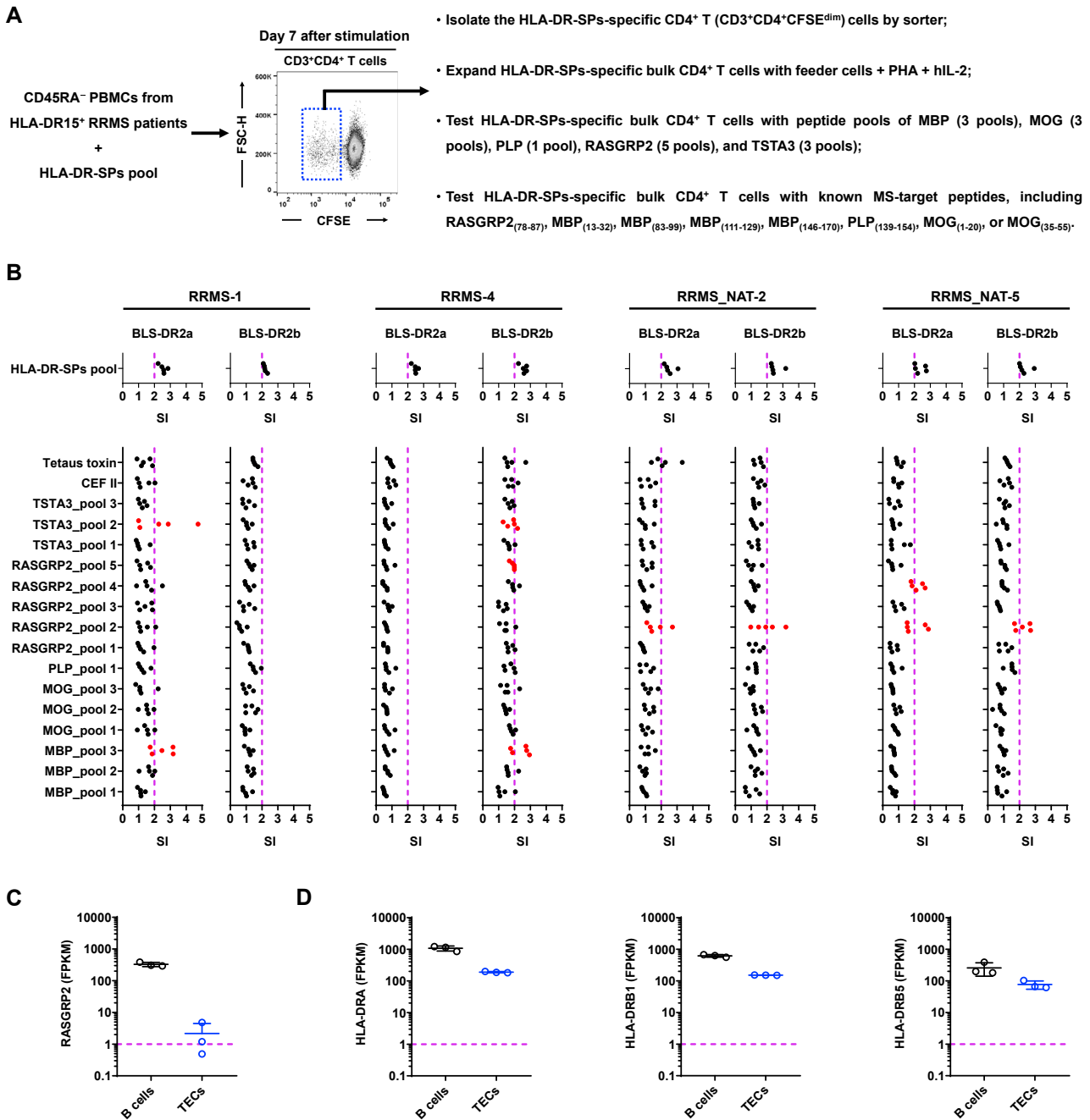
Figure S5. HLA-DR-SP-Specific CD4⁺ T Cells in MS Patients Respond to Peptides of MBP, RASGRP2, and TSTA3, Related to Figures 4 and 5 and Table S1

(A) Workflow diagram for the isolation and expansion of the HLA-DR-SPs-specific bulk CD4⁺ T cells in HLA-DR15⁺ RRMS patients.

(B) Proliferations of HLA-DR-SPs-specific bulk CD4⁺ T cells from HLA-DR15⁺ MS patients (n = 4) after co-culture with irradiated BLS-DR2a or BLS-DR2b cells as APCs and stimulation with peptide pools, including HLA-DR-SPs pool, myelin basic protein (MBP) peptide pools, myelin oligodendrocyte glycoprotein (MOG) peptide pools, myelin proteolipid protein (PLP) peptide pool, RASGRP2 peptide pools, and GDP-L-fucose synthase (TSTA3) peptide pools, for 7 days. Each stimulation was performed with 5 replicate wells. Proliferations were detected by ³H-thymidine incorporation assay, and the proliferation strength is depicted as SI. Groups with 2 or more positive wells are highlighted in red.

(C) The mRNA expression levels, expressed as FPKM (fragments per kilobase of exon model per million reads mapped), of RASGRP2 in TECs and blood B cells of HLA-DR15⁺ HDs. The purple dotted line indicates FPKM = 1. FPKM values above the purple dotted line were considered positive.

(D) The mRNA expression levels of HLA-DRA, HLA-DRB1, and HLA-DRB5 in TECs and blood B cells of HLA-DR15⁺ HDs.
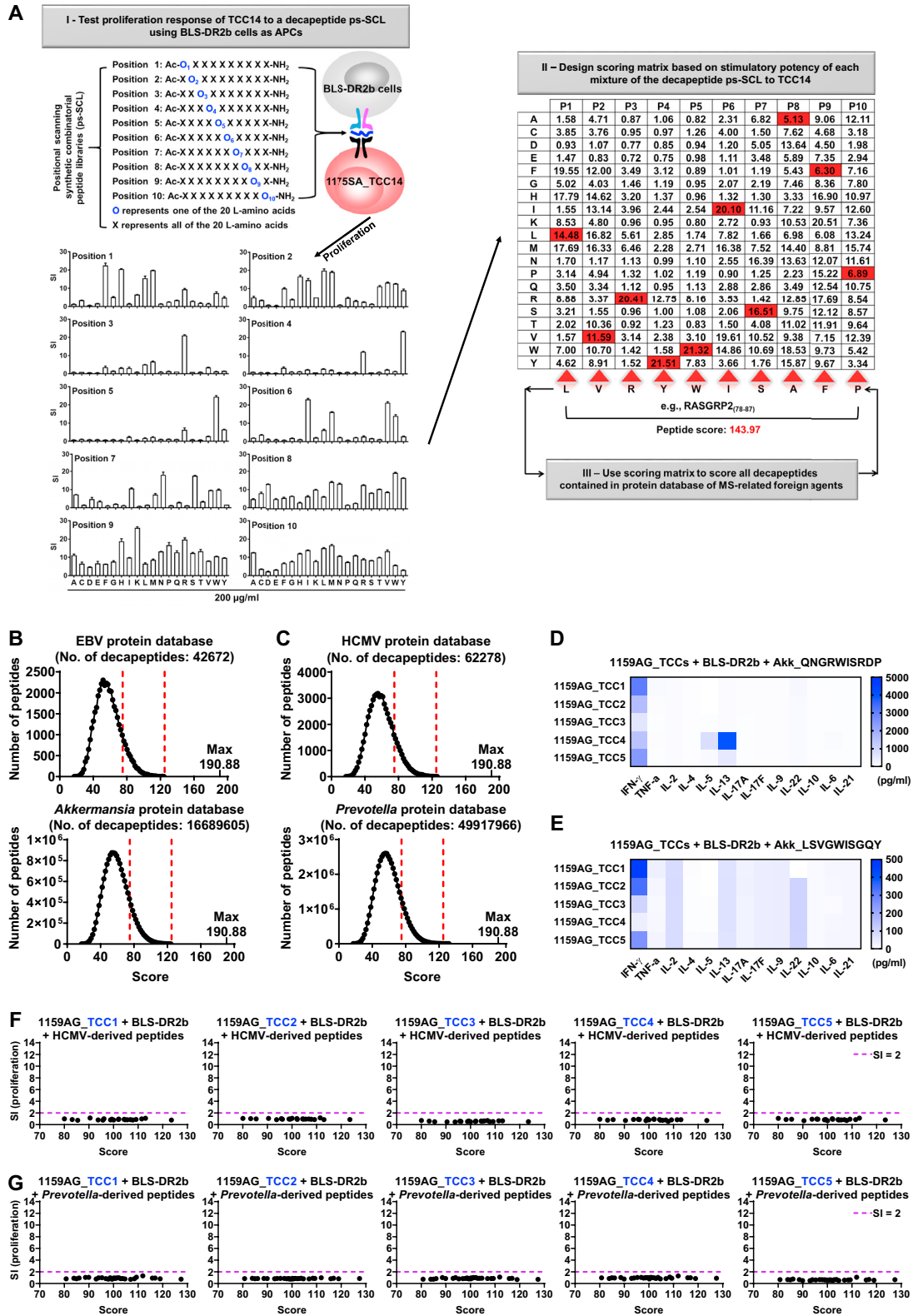
Figure S6. Prediction of Stimulatory Peptides from Foreign Agents for TCC14, Related to Figure 6 and Table S7

(A) Screening procedure for foreign agent-derived peptide ligand identification of TCC14 using positional scanning synthetic combinatorial peptide libraries (ps-SCL). (I) TCC14 was tested with all combinatorial decapeptide mixtures using irradiated BLS-DR2b cells as APCs. Proliferation responses were analyzed at day 3

(legend continued on next page)

by ^{3}H-thymidine incorporation assay. Proliferation strength is depicted as SI. (II) Mean responses from three repetitive experiments were used to generate a scoring matrix for optimal amino acid combinations of a potential peptide ligand. (III) The scoring matrix was used to screen the protein database of the foreign agents, and potential stimulatory decapeptides for TCC14 were selected based on a biometrical analysis.

(B-C) Score distribution of all decapeptides from MS-associated pathogens EBV and *Akkermansia* (B) as well as control pathogens HCMV and *Prevotella* (C). The red dotted lines indicate the score range for peptide selection.

(D) Concentrations of Th1/Th2/Th17-related cytokines in supernatants of the 1159AG_TCCs after co-culture with irradiated BLS-DR2b cells as APCs and stimulation with Akk_QNGRWISRDP for 3 days were detected by a bead-based immunoassay.

(E) Concentrations of Th1/Th2/Th17-related cytokines in supernatants of the 1159AG_TCCs after co-culture with irradiated BLS-DR2b cells as APCs and stimulation with Akk_LSVGWISGQY for 3 days were detected by a bead-based immunoassay.

(F-G) 1159AG_TCCs were tested with predicted decapeptides from HCMV (F) or *Prevotella* (G) using irradiated BLS-DR2b cells as APCs. Proliferation were detected by ^{3}H-thymidine incorporation assay after 3 days, and proliferation strength is depicted as SI.
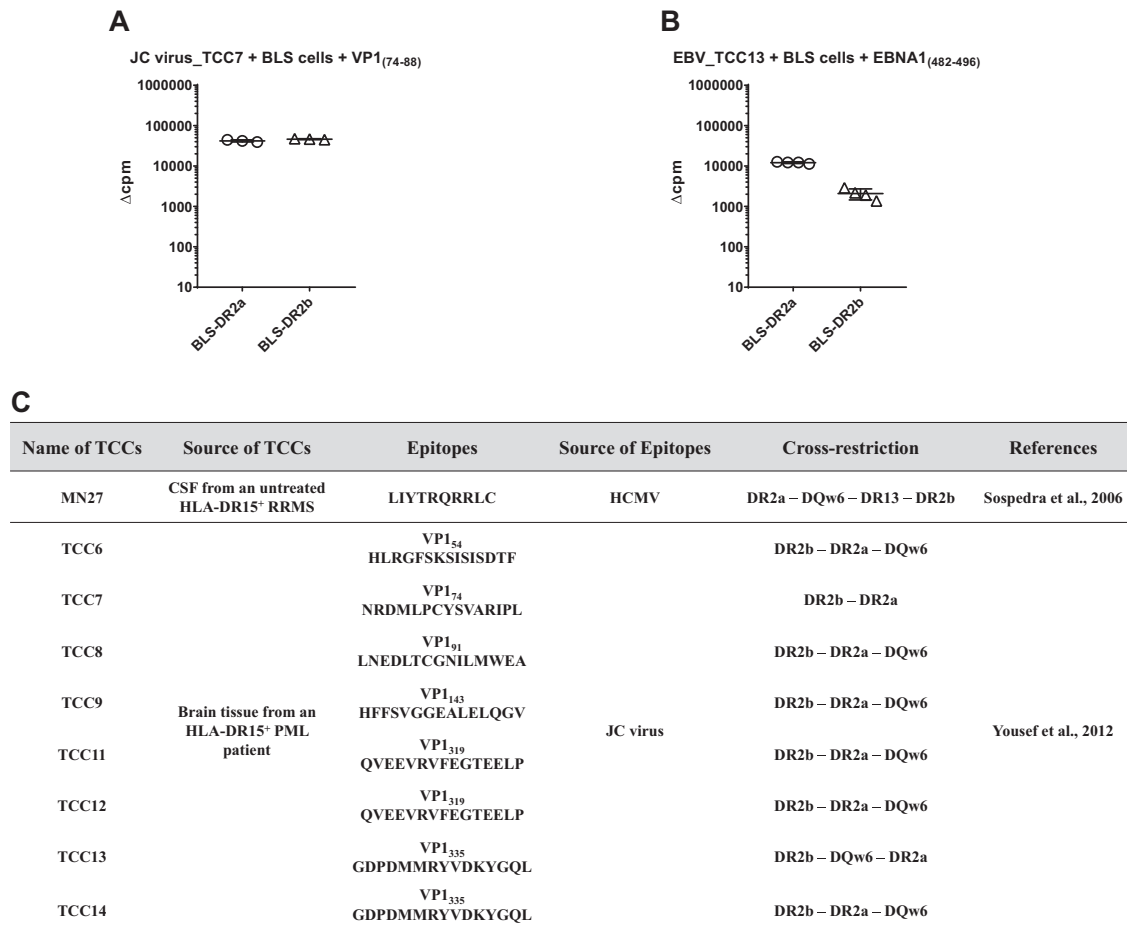
A

JC virus_TCC7 + BLS cells + VP1$_{(74-88)}$

B

EBV_TCC13 + BLS cells + EBNA1$_{(482-496)}$

C

Name of TCCs	Source of TCCs	Epitopes	Source of Epitopes	Cross-restriction	References
MN27	CSF from an untreated HLA-DR15+ RRMS	LIYTRQRRLC	HCMV	DR2a – DQw6 – DR13 – DR2b	Sospedra et al., 2006
TCC6		VP1$_{54}$ HLRGFSKSISISDTF		DR2b – DR2a – DQw6	
TCC7		VP1$_{74}$ NRDMLPCYSVARIPL		DR2b – DR2a	
TCC8		VP1$_{91}$ LNEDLTCGNILMWEA		DR2b – DR2a – DQw6	
TCC9	Brain tissue from an HLA-DR15+ PML patient	VP1$_{143}$ HFFSVGGEALELQGV	JC virus	DR2b – DR2a – DQw6	Yousef et al., 2012
TCC11		VP1$_{319}$ QVEEVRVFEGTEELP		DR2b – DR2a – DQw6	
TCC12		VP1$_{319}$ QVEEVRVFEGTEELP		DR2b – DR2a – DQw6	
TCC13		VP1$_{335}$ GDPDMMRYVDKYGQL		DR2b – DQw6 – DR2a	
TCC14		VP1$_{335}$ GDPDMMRYVDKYGQL		DR2b – DR2a – DQw6	

Figure S7. Virus-Specific TCCs from HLA-DR15+ MS Patients Show HLA Cross-restriction, Related to Figure 7

(A) John Cunningham (JC) polyomavirus-specific TCC7 from an HLA-DR15+ MS patient was co-cultured with irradiated BLS-DR2a or BLS-DR2b cells as APCs and stimulated with VP1$_{(74-88)}$ for 3 days. Proliferations were detected by ^{3}H-thymidine incorporation assay. Δcpm indicates the cpm value above the no peptide control.

(B) EBV-specific TCC13 from an HLA-DR15+ MS patient was co-cultured with irradiated BLS-DR2a or BLS-DR2b cells as APCs and stimulated with EBNA1$_{(482-496)}$ for 3 days. Proliferations were detected by ^{3}H-thymidine incorporation assay.

(C) Virus-specific TCCs from HLA-DR15+ MS patients reported before show HLA cross-restriction by DR2a and DR2b when stimulated with their cognate HCMV or JC polyomavirus peptides.